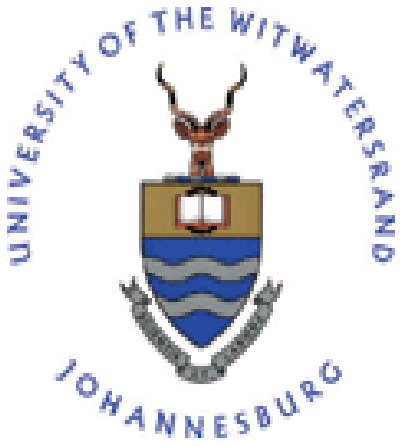

Numerical Modelling of High Vacuum Columns for Life Assessment and Failure Prevention

Lethukuthula Magasela
(Student number: 1109770)

School of Mechanical, Industrial and Aeronautical Engineering

University of the Witwatersrand

Johannesburg, South Africa.

Supervisors: Professor J.P. Nobre

A research report submitted to the Faculty of Engineering and the Built Environment, University of the Witwatersrand, in fulfilment of the requirements for the degree of Masters in Engineering.

Date: 20 May 2018

Declaration

I declare that this Research Report is my own, unaided work. It is being submitted for the Degree of Master of Science in Engineering at the University of the Witwatersrand, Johannesburg. It has not been submitted before for any degree or examination at any other University.

(Signature of candidate)

----------day of ----------20----------in----------

Acknowledgements

I would like to acknowledge some of the individuals that have made it possible for me to write this report on numerical modelling of high vacuum columns for life assessment and failure prevention. To my supervisor, Professor J.P. Nobre, thank you for pushing the envelope and allowing to grow in field of mechanical engineering, specifically on the effect of corrosion on pressure vessels and to understand the various finite element modelling techniques that may be utilised to define margins of safety.

To my organisation, SAPREF, thank you for allowing me to conduct this research on such highly complicated structures within the plant. This research benefits both my personal development and capability improvement within the organisation, more importantly this ensures that plant personnel are safe and economic benefits in averting an unplanned outage. Within my organisation, I would like to acknowledge the Inspection team which keeps all historical records of equipment especially the unit inspectors and the materials and corrosion teams for their advices on some of the key technical aspects associated with high vacuum columns.

I would like to thank the University in providing the necessary resources especially research papers available on the library via the internet. This has allowed for the material contained in this report to be up to date in terms of the latest technological tools, for example, the use of Ansys modelling software in the technical analysis of the structure.

Finally, I would like to acknowledge my family, i.e. wife and two kids. I know at times it seemed I was not there but it was necessary for the future wellbeing. Thank you for all the support.

Abstract

High vacuum towers in the petrochemical industry are common especially in crude refineries. They operate in deep vacuum, usually around 98kPa and very high temperatures in the region of 400℃. They perform a critical role in the crude processing plants in which vaporised crude oil from heaters is fed into these vessels to produce products such as vacuum residue, heavy vacuum gas oil, light vacuum gas oil and so forth under this deep vacuum environment.

This specific vacuum tower under review suffered severe localised internal corrosion on the upper section just above the conical section. The conical section of the column together with the bottom section are constructed from carbon steel which is clad with stainless steel to mitigate against naphthenic acid corrosion attack. Unfortunately, the top section does not have this cladding even though temperature profile in the region indicated that naphthenic acid corrosion would still be active.

Literature review undertaken revealed the various forms of failures under corrosion, the most prominent being stress corrosion and corrosion fatigue. It was established that there were not cracks in the structure during inspections and that the most likely failure mechanism under corrosion would be buckling of the structure due to the negative internal pressure and the weight of the structure above the local thin area.

A numerical model was developed to simulate behaviour of the structure under all the applicable loads with the different scenarios being imposed onto the model, for example, varying the thickness of the thinned region to estimate failure. The predicted remaining life was only 18 months from the last inspection where buckling failure is expected to occur at a thickness less than 6.7mm.

Based on the results, a complete overhaul of the maintenance strategy is recommended which include immediately using on stream measuring techniques to predict wall thickness, review corrosion control documents to ensure proper material selection to prevent naphthenic acid corrosion, develop inspection strategies for high vacuum towers based on actual data and unique to each piece of equipment and finally ensure crude diet selection is supported by a technical review on the impact to process equipment.

In conclusion, life and failure prevention recommendations are specified to achieve objective.

Keywords

High vacuum columns

Stress corrosion

Finite element modelling

Naphthenic acid corrosion

Buckling

Table of Contents

List of figures

List of tables

Nomenclature

Abbreviation	*Expansion*
SAPREF	South African Petroleum Refineries
BS	British Standard
ASME	American Society of Mechanical Engineers
ASTM	American Society for Testing Materials
PD	Published Document
API	American Petroleum Institute
FCCU	Fluid Catalytic Cracking
FPU	Feed Preparation
CDU	Crude Distilling
DWO	Dirty Wash Oil
FEM	Finite Element Modelling
TBM	Time-based maintenance
CBM	Condition-based maintenance
OMUTDE	Oil movements, utilities, tankage & despatch
LVGO	Low vacuum gas oil
MVGO	Medium vacuum gas oil
HVGO	High vacuum gas oil
SS	Stainless steel
NAC	Naphthenic acid corrosion
TAN	Total acid number
RCM	Reliability centred maintenance
LEFM	Linear elastic fracture mechanics
SANS	South African National Standard
SCL	Stress classification line
PER	Pressure Equipment Regulations
RBI	Risk Based Inspection

INTRODUCTION

Purpose of study

This study forms part of the requirements to fulfil the Master of Science in Mechanical Engineering (MSc 50/50) programme at the University of the Witwatersrand. The research report deals with the development of finite element models to analyse the structural integrity of high vacuum columns, considering the main degradation mechanisms that prevail in petrochemical industry, in particular, the corrosion phenomena in high vacuum columns. These corrosion phenomena lead to the thinning of the vacuum columns walls, with a considerable effect on the reduction of its structural integrity and, consequently, can lead to its final catastrophic failure. Therefore, this study aims to develop numerical models to predict limits of utilization of these vessels, regarding its structural strength, to avoid permanent damages or complete failures due to plastic collapse and buckling. The numerical models to be developed will certainly be an important tool to prevent failures, enabling to propose plans for the preventive maintenance of this very important equipment for the petrochemical industry.

Research Background/Context

For developing the necessary numerical models, a full bibliographic revision is carried out to better understand the petrochemical refinement of the crude oil and, in particular, the chemical reactions and products produced in high vacuum towers. This revision will enable to understand the different forms of corrosion and how to control the corrosion phenomena on the materials used to manufacture these vessels. All aspects related with the main parameters involved in the design process of this equipment will be reviewed for a better assessment of its structural integrity. Particular attention will be paid to the main standards usually followed to determine the mechanical strength of high vacuum towers. The mechanical behaviour of materials and its relation with the mechanical loads involved, such as pressure, wind loads and weight, will allow to determine the best numerical approach to be followed, considering the main failure mechanisms involved, such as, plastic collapse, buckling, corrosion and fatigue. In addition the different types of maintenance will be revisited as a way to implement an appropriate preventive maintenance plan for the equipment under study. First important findings will be described in detail in the following Literature Review section.

Research Motivation

In the past five years, Shell & BP South African Petroleum Refineries Pty (Ltd) (SAPREF) has conducted emergency repairs on two of its high vacuum towers, due to a lack of in-house knowledge to properly propose reliable maintenance plans. These maintenance plans require the numerical evaluation of the structural strength of these towers, regarding the different failure mechanisms, based on the latest inspection data. Without reliable maintenance plans, the risk of plant unavailability, due to unpredicted maintenance interventions, or, worse, the risk of catastrophic failures, can imply, either huge financial costs or loss of human lives. Therefore the numerical modelling to be conducted will certainly contribute to improve preventive maintenance plans of high vacuum columns plus safeguard risk of injury/loss of human lives. These preventive maintenance plans will further be established based on a periodic maintenance plan (TBM) or in a predictive maintenance plan (CBM), depending on the achievements of the study to be carried out.

Plant Description

SAPREF is a crude oil refinery located on the east coast of South Africa in the city of Durban. It is the largest crude oil refinery in Southern Africa and processes about 180000 barrels of crude oil per day. The first units of the refinery were commissioned in 1964. Refinery ownership is a joint venture between Shell South Africa Refining and BP Southern Africa. Main refinery products include petrol, diesel, jet fuel, paraffin, marine fuel oil, bitumen and so many other products. The site is further subdivided into zones, i.e. South Zone, Central Zone, North Zone, OMUTDE and Island View, where all the blending and storage of semi-finished and finished products is done. Island View is located at the Durban harbour terminal. Overall layout of the refinery is shown on Figure 1 below:

Figure 1 Overall refinery layout (Permission by SAPREF HR Department)

Process Description

The Crude Distillation Unit (CDU) is usually the first unit in a refinery in which crude oil is received from storage and pre-heated before being pushed through the main heater in order to increase the crude oil temperature to about 350℃. This vaporised crude enters an atmospheric column in which distillation takes place. One of the distillates, atmospheric residue, becomes feed into the high vacuum column. Typical process is shown on figure 2.

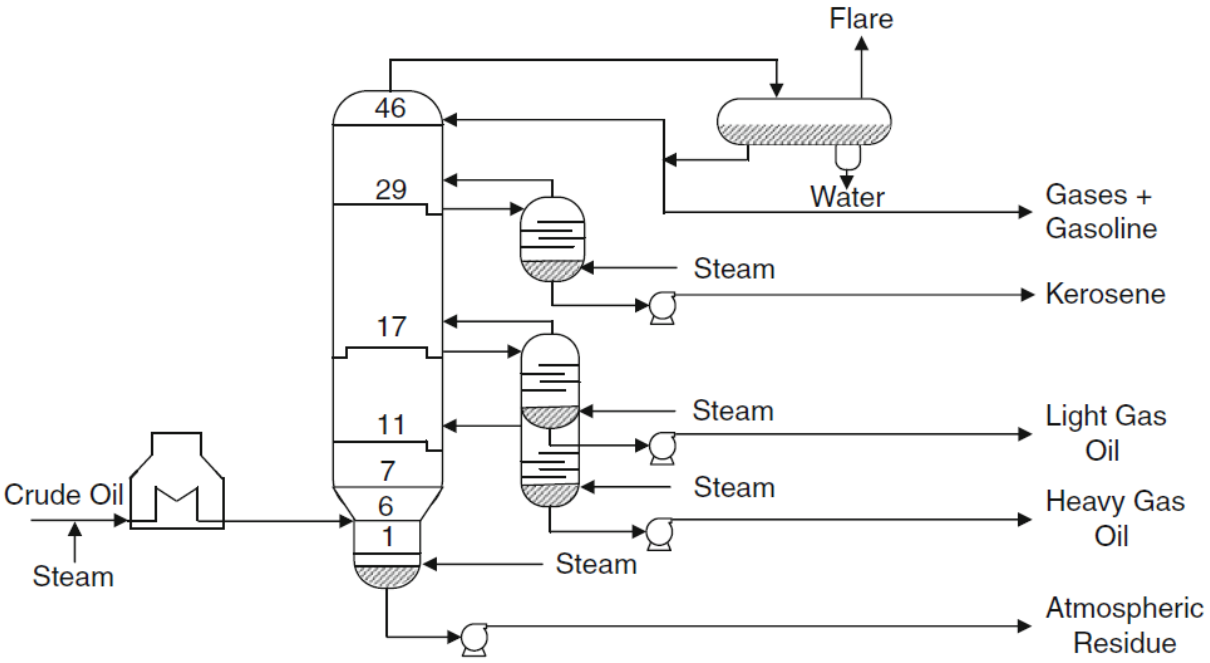

Figure 2 Typical arrangement for crude distilling unit [1]

The high vacuum column, C7701, is in the Feed Preparation Unit (FPU) within the south zone plot at SAPREF. The purpose of the high vacuum column is to produce distillates such as light vacuum gas oil (LVGO), medium vacuum gas oil (MVGO) and high vacuum gas oil (HVGO). The vacuum gas oils are used to feed downstream units such as the Fluid Catalytic Cracking Unit (FCCU). This is shown in detail on figure 3.

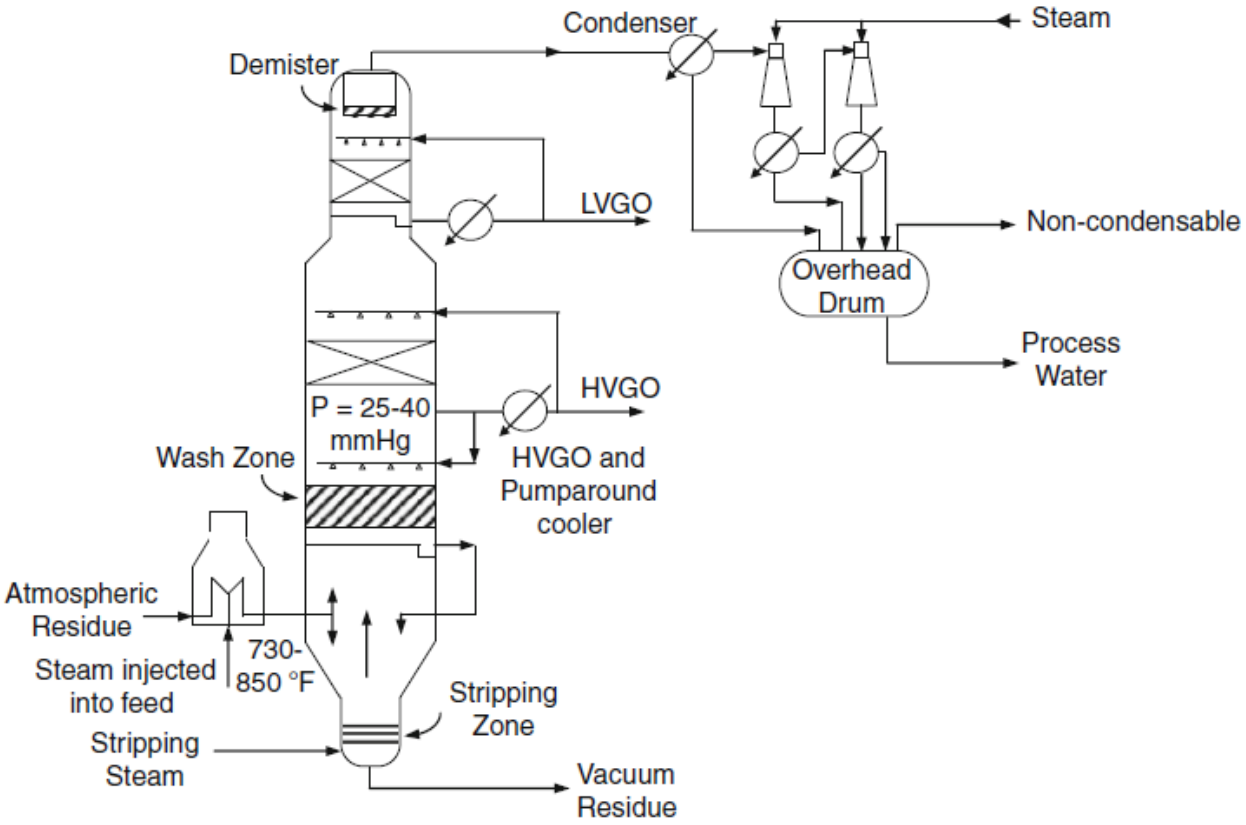

Figure 3 Typical arrangement of high vacuum process [1]

Problem statement

During a statutory inspection of the high vacuum tower, C7701, in September 2013 it was noted that a section above the swage (conical section) has severely thinned and that maybe structural integrity is compromised. Figure 4 depicts the tower general arrangement drawing.

This high vacuum tower was commissioned in 1976 designed in accordance to the BS1515 British pressure vessel code and applicable Vessels Under Pressure Regulation at the time. Design parameters are listed below:

- Design pressure internal/external 1.67/-1.013 barg
- Design temperature top/bottom 350°C/405°C
- Main material of construction carbon steel (bottom section clad with SS)
- Medium hydrocarbons
- Nominal wall thickness 19 mm
- Outside diameter top/bottom 6400mm/8500mm
- Vessel height 31800mm

Top section is the section above the swage and the bottom section is from the swage down. In 2004 the top section was replaced due to internal corrosion but a section of 1250 mm above swage was not replaced.

The September 2013 report indicated wall loss of the cylindrical section above the swage up to 10.8 mm, this was very close to 50% wall loss from original thickness of 19 mm. Further inspection data using a c-scan technique was carried out in June 2015 and this will form part as an input into numerical modelling. In essence, there is an integrity risk on the section above the swage that needs to be investigated in order to understand the stress states and compare to failure criterion. This is due to internal corrosion that will be further discussed in the literature survey.

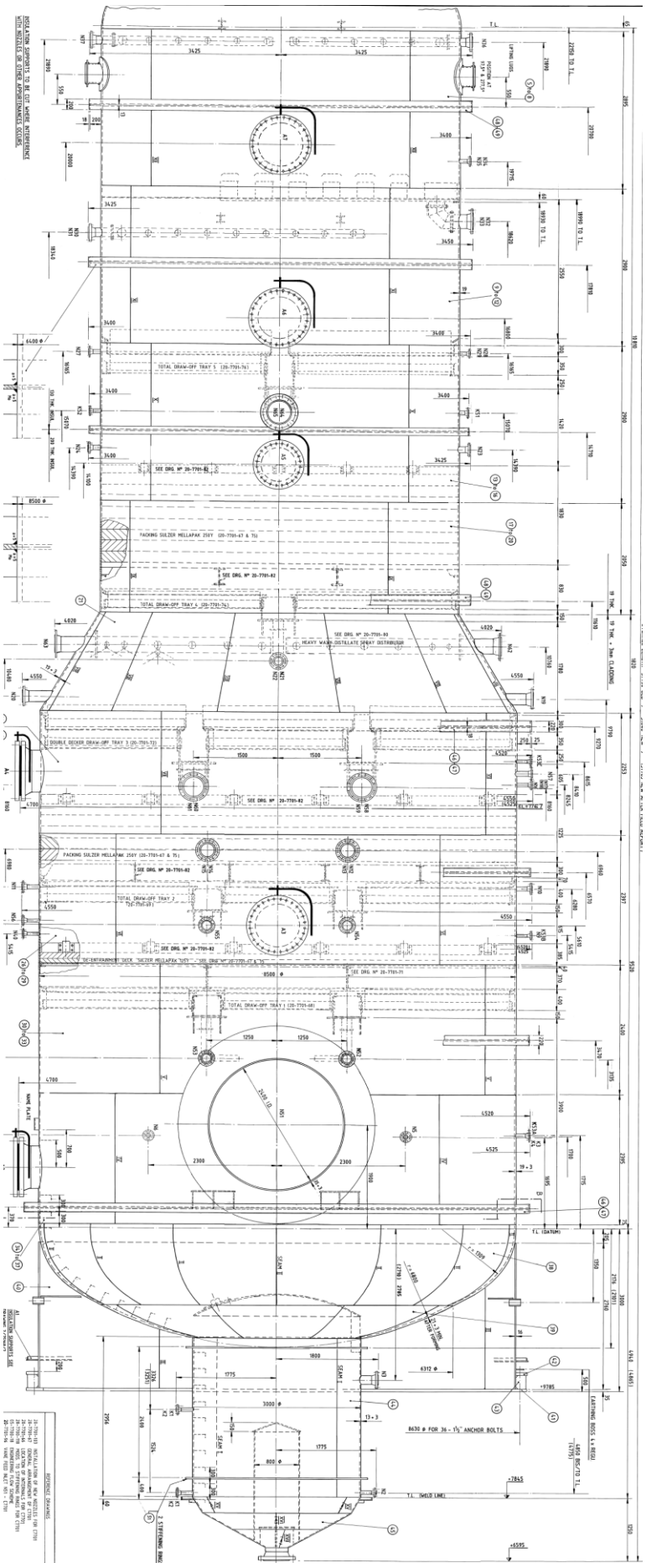

Figure 4 High vacuum tower *C7701 general arrangement drawing*

RESEARCH QUESTIONS/HYPOTHESIS

Below are the questions the research project seeks to cover:

a) What is the effect of the various crude diets on design life of high vacuum columns?
b) What is the relationship between corrosion and mechanical strength behaviour?
c) What are the numerical models applicable to high vacuum columns when assessing for plastic collapse, buckling and so forth?
d) How to improve the reliability of high vacuum columns?

RESEARCH OBJECTIVES

This study aims to develop numerical models to predict limits of utilization of high vacuum columns, to avoid permanent damages or complete failures due to plastic collapse, buckling and unstable fracture. The numerical models to be developed will certainly be an important tool to prevent failures, enabling to propose plans for the preventive maintenance of this very important equipment for the petrochemical industry.

RESEARCH METHODS

Literature review was conducted to establish all theory that relates to failure prevention of the high vacuum columns due to corrosion and the numerical modelling techniques available to predict failure. In the research with regards to corrosion, research from various sources including the API confirmed the active corrosion mechanisms that the high vacuum columns undergo, i.e. Naphthenic Acid Corrosion. The various sources also highlighted numerous factors that may be put in place to mitigate from this form of corrosion including use of alloyed steels, avoiding certain crude diets due to their sulphur contents and also making use of cladded steels.

The research than shifted focus towards the behaviour of materials under the identified corrosion mechanisms. Literature on stress corrosion highlighted the importance to establish a threshold stress parameter under which crack propagation will not occur when a load is applied onto a material in a corrosive environment. The research further indicated that there have been advancements in the prediction of crack growth with the use of the crack growth to stress intensity factor curves. This research is of particular importance when assessing pressure vessels with crack like defects for life assessments.

Further to behaviour of materials under corrosion, more research was uncovered which relates to fatigue corrosion in which a structure is subjected to cyclic loading under a corrosive environment. This is quite a major concern on pressure vessels in which crack like indications have been identified during an inspection. Fortunately the high vacuum column is not operating under cyclic loading and upon inspection no crack like indications were found.

In the unpacking of NAC active on the high vacuum column it became very clear that this particular corrosion mechanism results in general wall of metal and the structure becomes compromised due to reduced wall loss rather than crack formation. This was confirmed with the inspection results. Based on the inspection results, numerical modelling software was used to predict failure of the high vacuum column. Finally, the research focused on the maintenance theories and their differences, i.e. breakdown or reactive maintenance and preventive maintenance. It was found that the current maintenance strategy is not reliable to fully predict failure of the high vacuum column. The current strategy is more time based and lacks some key tools within the predictive maintenance realm. Furthermore, the remaining life assessment based on corrosion rates is neglected due to the periodic maintenance strategy that was adopted.

LITERATURE REVIEW

Pressure Vessel Design

In the petrochemical industry, there are codes that have been developed to ensure the safety of plant personnel due to tragic events that have occurred in the past. The most common codes of construction include American Society of Mechanical Engineers (ASME VIII-1) from USA, Published Document (PD5500) from the UK, AD Merkblatt from Germany and so forth. In these codes safety factors are established and must be maintained in the design of new pressure vessels. The calculation procedures defined in these codes are based on fundamental strength of materials.

In the ASME VIII-1 design code for example, allowable stress properties are established through the application of a safety factor of 3.5 onto the yield strength of a material at room temperature. Therefore, when thickness calculations are performed, any stress values greater than the defined allowable stress are not acceptable.

Pressure vessel failure categories are listed below in which any form of failure in a pressure vessel can be attributed into [2]:

1. *Material*, this is about the selection of suitable materials for the service and any defects that maybe inherent in the material from the manufacturing processes involve
2. *Design*, inaccurate design method/procedure, incorrect design data specified, inadequate shop testing
3. *Fabrication*, poor quality control, improper or insufficient fabrication procedures including welding, heat treatment or forming methods
4. *Service*, change of service condition, inexperienced operations and maintenance personnel, upset conditions

Types of pressure vessel failures are described in detail below:

1. *Elastic deformation*, elastic instability or elastic buckling, vessel geometry, and stiffness as well as properties of materials are protection against buckling
2. *Brittle fracture*, can occur at low or intermediate temperatures
3. *Excessive plastic deformation*, this involves review of primary and secondary stress limits which are intended to prevent excessive plastic deformation and incremental collapse
4. *Stress rupture*, creep deformation as a result of fatigue or cyclic loading

5. *Plastic instability*, incremental collapse which is cyclic strain accumulation
6. Low cycle fatigue , *high strain level*, which is strain governed and occurs mainly in lower strength/high ductile materials (also related with the stress-strains due to thermal variations)
7. *Stress corrosion*, this is mainly about formation of chlorides leading to stress corrosion cracking in stainless steels and caustic service in carbon steels
8. *Corrosion fatigue*, occurs when corrosive and fatigue effects occur simultaneously.

Corrosion phenomena

Corrosion is defined as the deterioration of a metal or its properties because of a reaction with its environment [3]. The many forms of corrosion are listed below,

- General corrosion
- Localized corrosion (pitting, crevice and filiform)
- Galvanic corrosion
- Environmental corrosion cracking
- Velocity effect corrosion
- Intergranular corrosion
- Dealloying
- Fretting corrosion
- High temperature corrosion

Some examples of indirect consequences related to corrosion include leaks, structural collapse, safety, product contamination and so forth.

Corrosion is an electrochemical reaction except for high temperature corrosion, therefore for corrosion to occur there must be an electron path (electrolyte), at the anodes electrons are given off which travel through the metal and are consumed at the cathode.

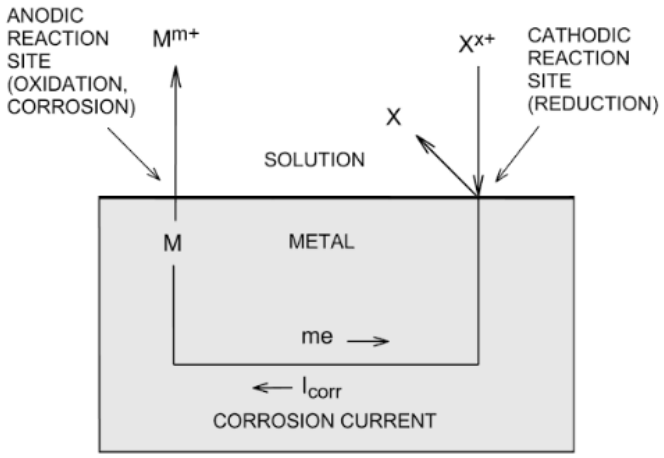

Figure 5 Basic corrosion process [4]

Corrosion in high vacuum columns

The API 571 specification outlines various degradation mechanisms related to the various units found in oil refineries. Snapshot of the various mechanisms is shown below:

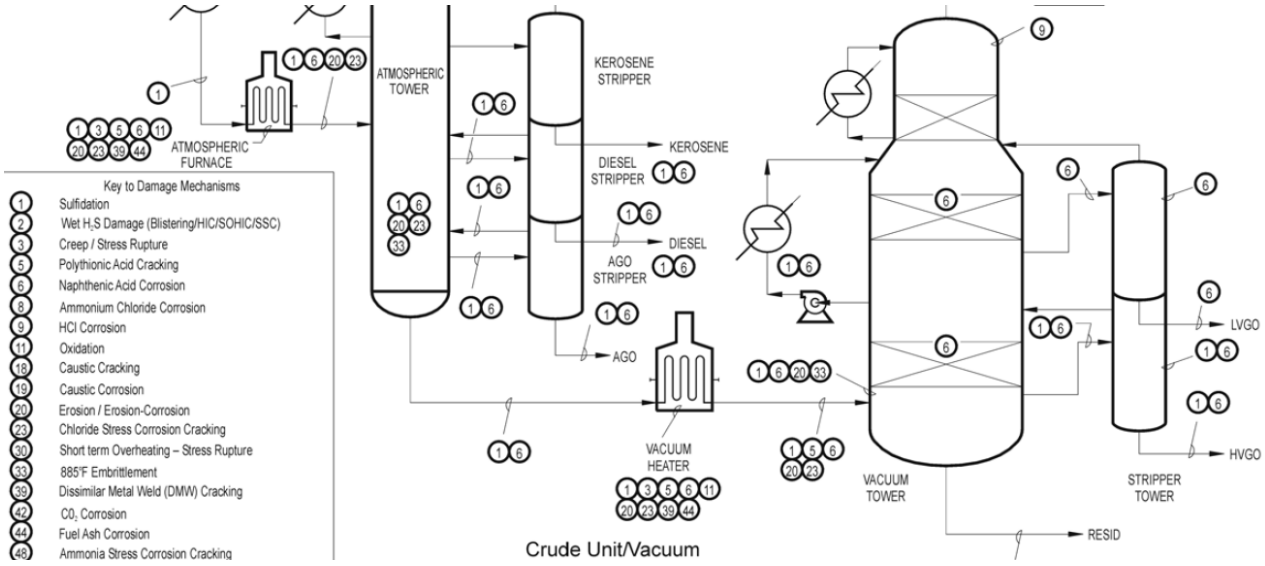

Figure 6 Primary damage mechanisms in vacuum towers [5]

In accordance with Figure 6, the high vacuum column suffers predominantly from naphthenic acid corrosion (NAC). NAC is a form of high temperature corrosion in which products produced contains traces of naphthenic acids.

According to [5], some of the critical factors related to NAC are:

- NAC is a function of the naphthenic acid content (neutralization number), temperature, sulfur content,velocity and alloy composition.
- Severity of corrosion increases with increasing acidity of the hydrocarbon phase.
- Neutralization number or Total Acid Number (TAN) is a measure of the acidity (organic acid content) as determined by various test methods such as ASTM D-664. However, NAC corrosion is associated with hot dry hydrocarbon streams that do not contain a free water phase.
- The Total Acid Number (TAN) of the crude may be misleading because this family of acids has a range of boiling points and tends to concentrate in various cuts. Therefore, NAC is determined by the acidity of the actual stream not the crude charge.
- The various acids which comprise the naphthenic acid family can have distinctly different corrosivity.
- No widely accepted prediction methods have been developed to correlate corrosion rate with the various factors influencing it.
- Sulfur promotes iron sulfide formation and has an inhibiting effect on NAC, up to a point.
- Naphthenic acids remove protective iron sulfide scales on the surface of metals.
- NAC can be a particular problem with very low sulfur crudes with TAN's as low as 0.10.
- NAC normally occurs in hot streams above 218℃ but has been reported as low as 177℃. Severity increases with temperature up to about 400℃, however, NAC has been observed in hot coker gas oil streams up to 427℃
- Naphthenic acids are destroyed by catalytic reactions in downstream hydroprocessing and FCCU units.
- Alloys containing increasing amounts of molybdenum show improved resistance. A minimum of 2% to2.5% is required depending on the TAN of the whole crude and its side cuts.
- Corrosion is most severe in two phase (liquid and vapor) flow, in areas of high velocity or turbulence, and in distillation towers where hot vapors condense to form liquid phase droplets.

NAC mainly affects carbon steel, low alloy steels, 300 series stainless steels, 400 series stainless steels and nickel base alloys.

NAC may be prevented through metallurgy upgrades (materials with more Molybdenum content), blend crude to reduce TAN or utilization of chemical inhibitors.

In order to prevent NAC inside C7701, the bottom section including the conical section of the column is clad with 410 SS. The section that is compromised, which is above the conical section, has suffered aggressive NAC since the material is carbon steel without any form of cladding. Operating temperatures around this region are around 230 to 276 ℃, these are favourable conditions for NAC to occur. This may have been accelerated by the change in crude diet due to a low TAN, around 0.2.

Mechanical Behaviour of materials subjected to corrosion

Stress Corrosion

Stress corrosion is a material's damaging process caused by the combined action of a corrosive medium and an applied static load. The corrosive environment facilitates the crack initiation, which, in certain cases, may lead to the complete failure of the component or structure. The susceptibility to stress corrosion depends on several variables and properties of the material, such as its chemical composition, the thermal treatments, its microstructure and the temperature [10].

A main parameter that can be used to predict the material behaviour to stress corrosion is the so-called threshold stress to stress corrosion. This stress can be defined by the level of ***s***tress below which no rupture is observed by stress corrosion as shown on figure 7 [6**]**.

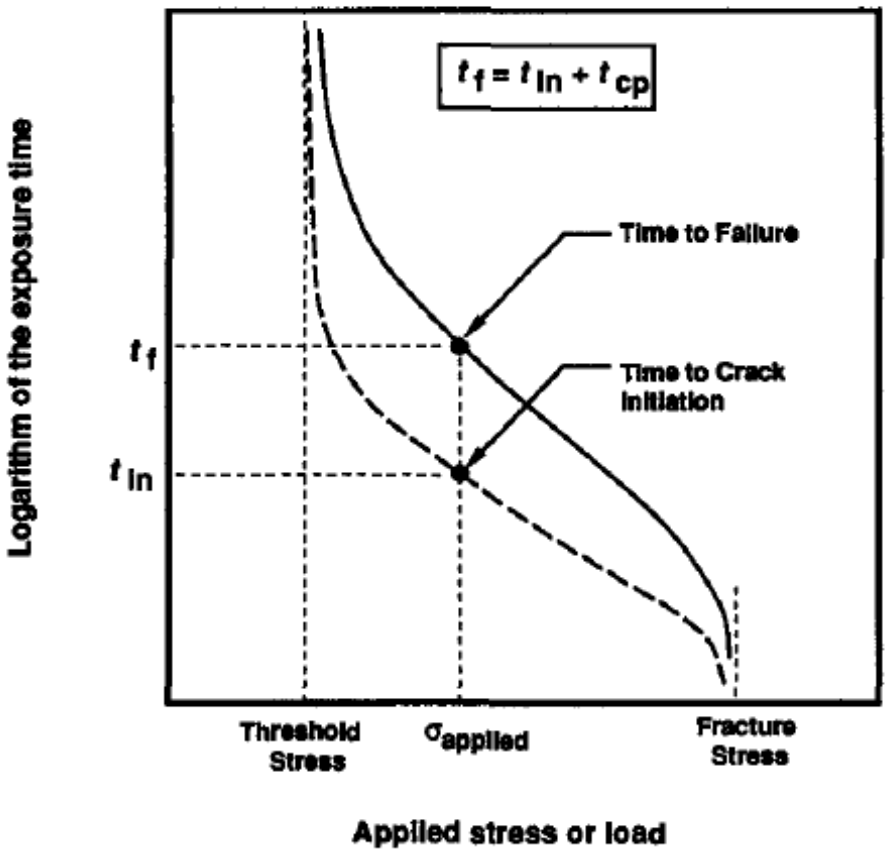

Figure 7 Applied stress vs. time to rupture of a specimen subjected to stress corrosion [6]

In the experiment shown on figure above, time to failure is plotted against the applied stress. It is noted that time to failure increases rapidly with less applied stress to a point defined as the threshold stress, in which crack initiation approaches infinity. This figure provides essential information necessary for inspection interval specification and calculation of maximum stress that may be applied on a material without being concerned by failure due to stress corrosion.

The major difficulty to use this parameter is related with the strict definition of the applied stress, since the stress corrosion process develops at localized points, which can either be defects or pitting corrosion bites. The process is thus controlled by the stress at these points and not by the nominal stress applied to the part. The two stresses, the nominal and the local one, can be very different, which can lead to significant analysis errors.

Alternatively to this approach, the Linear Elastic Fracture Mechanics (LEFM) can be used, since the values of the stress intensity factor, K, related with the stable crack propagation are lower than those related with unstable crack propagation, which lead to unstable fracture.

Based on the concept of similarity with the fatigue process, the so-called curves da/dt-K can be used to analyse the material's behaviour to stress corrosion. These curves can be determined for each material and environmental conditions using experimental methods very similar to those used to determine the well-known da/dt-ΔK curves, which describe the crack propagation under cyclic fatigue loading. Figure 8 shows a typical setup for stress corrosion analysis.

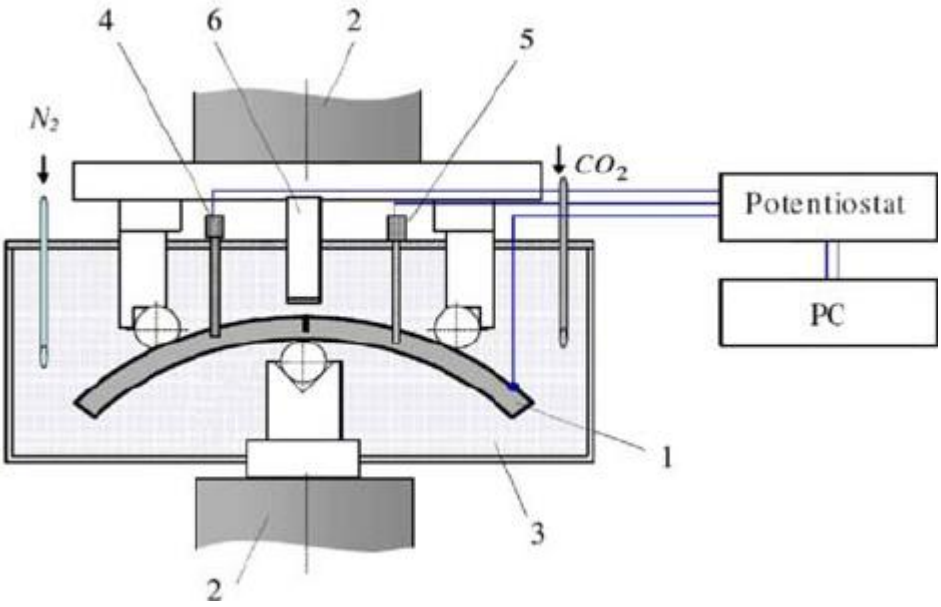

Figure 8 Schematic view of 3-point bending test rig for stress corrosion analysis (electrolysis cell): 1 - pre-cracked test specimen, 2 - loading device of testing machine: 3 - corrosion cell: 4 - pH electrode: 5 - reference calomel electrode: 6 - auxiliary electrode.

The region of the slit is brought into contact with the medium environment and subjected to a static tensile load. In most of material - medium environmental systems, the curve da/dt-K presents three propagation regimes 1, 2 and 3. In regime 1 the speed of propagation depends heavily of K, having a minimum value, called propagation threshold to stress corrosion, or threshold stress intensity for propagation of stress corrosion, K_{1SCC}, below which the propagation speed is less than 10^{-7}m/s. In regime 2 the propagation speed is, in general, constant and independent of the stress intensity factor, K. Finally, in regime 3 there is a significant acceleration, especially when K approaches the critical value K_{1c} or K_c, the fracture toughness [7]. Figure 9 [6] shows the typical da/dt-K curves.

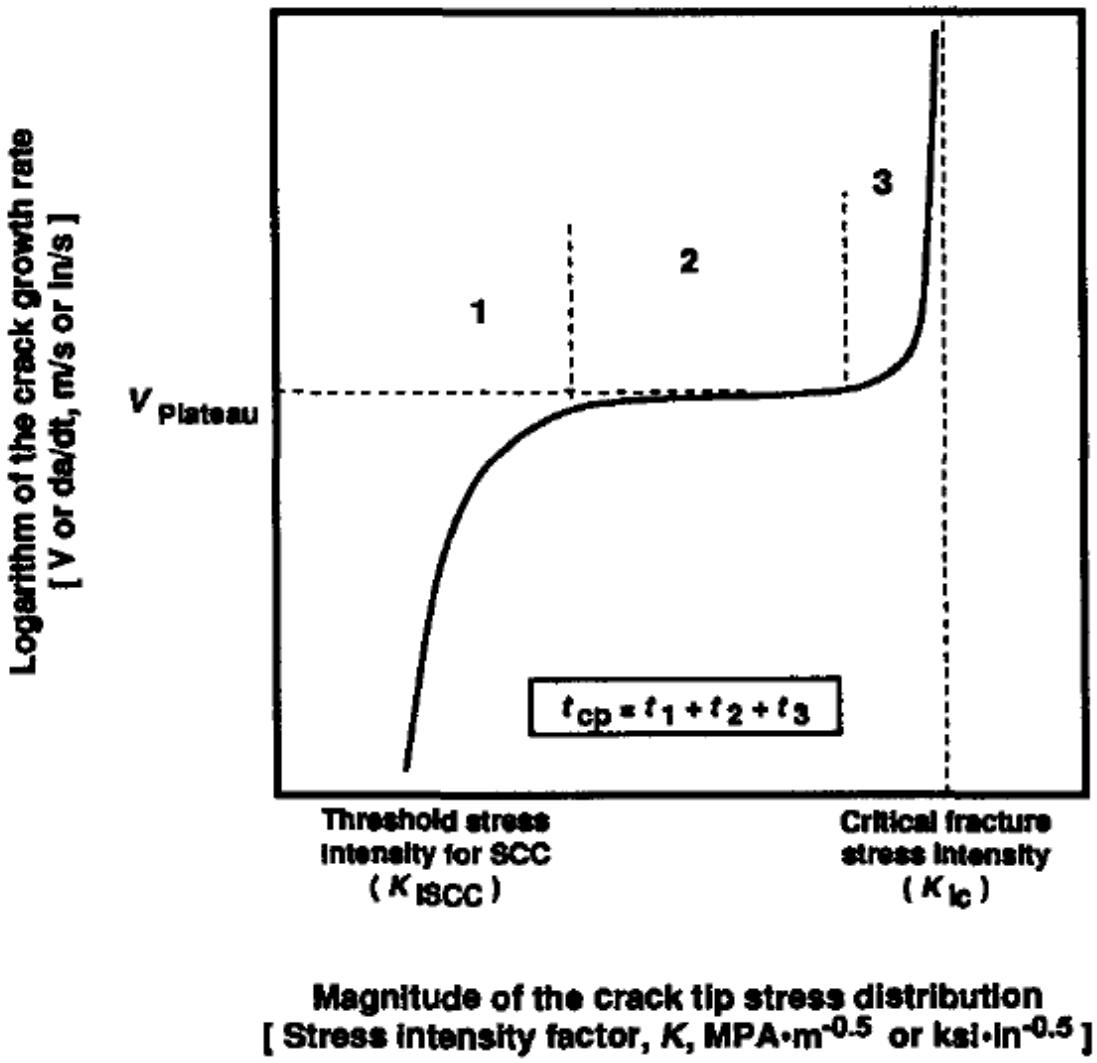

Figure 9 Crack propagation rate as a function of stress intensity [6]

The use of the da/dt-K curves allows an adequate selection of materials and important influence technological parameters. Main variables to take into account:

- Direction of the applied load (particularly important in the aluminium alloys):
- Environment (composition, concentration and temperature):
- Heat treatment:
- Residual stresses:
- Composition of material, etc.

Fatigue Corrosion

Corrosion fatigue occurs when a metal is subjected to corrosive environment together with alternating stresses. This results in cracks formation which often initiate at high stress concentrations such as pits. Susceptibility of metals to corrosion fatigue mainly depends on corrosive environments that promote pitting or localised corrosion, presence of cyclic stresses such as thermal stresses, vibration or expansion.

Failure of metals due to corrosion fatigue may occur well below the endurance limit [7], hence there is no fatigue limit load.

An example of typical fatigue load frequency is shown in Figure 10, where data is presented in the form of ΔK (stress intensity factor range). It is worth noting that the maximum stress intensity factor (K_{max}) plotted is below critical value, $K_{Iscc,}$ approximately 55 MPa. The fatigue crack growths at low frequencies are much higher than those at higher frequencies, this confirms that in corrosion fatigue the corrosive environment has a major impact.

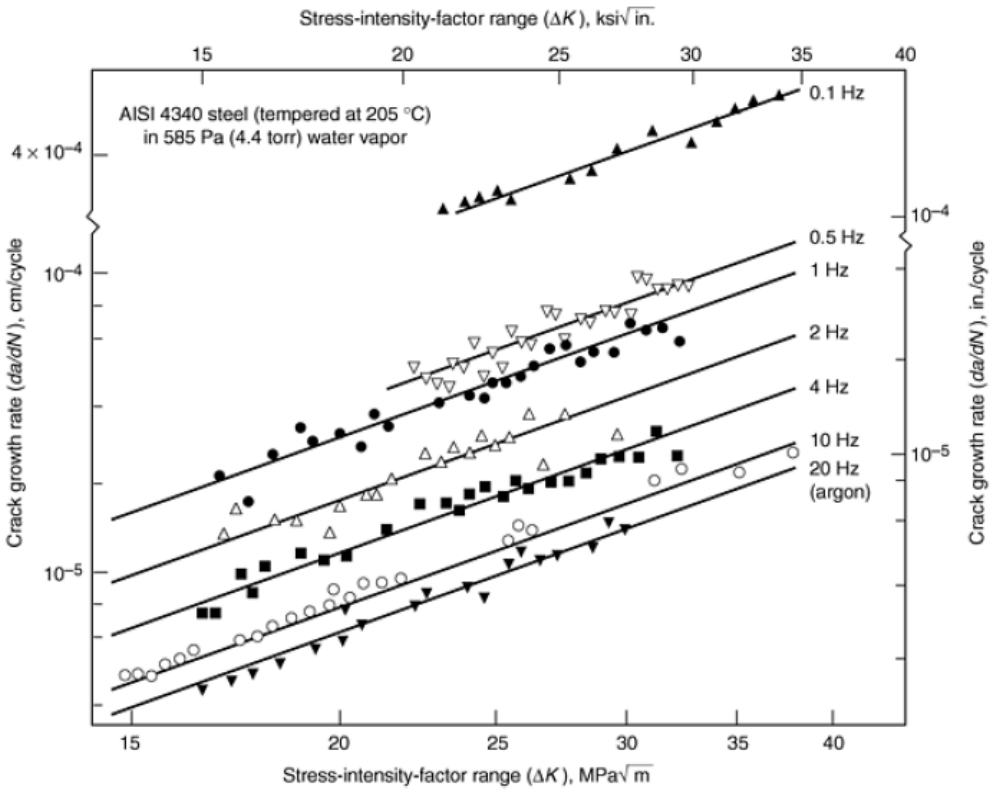

Figure 10 Typical fatigue crack growth of an alloy steel at room temperature [8]

Failure Theories

Maximum Distortional Energy

In this theory it is specified that yielding will occur when the distortional strain energy reaches that value which causes yielding in a simple tension test, this theory addresses ductile, isotropic materials. This theory is more comprehensive than maximum shear stress theory in that it considers energy caused by shear deformations in three dimensions. Maximum distortional energy is also less conservative than maximum shear stress, i.e. yielding at 0.5 yield vs. 0.557 yield. This theory was developed by R von Mises around 1913 [2].

Numerical modelling

In order to model various failure modes, different ANSYS models will be developed in order to accurately predict failure of the structure. There are some very key steps in developing the model which are necessary, these are noted below:

Specification of material properties

Table 1 Vacuum column material properties

	Material	Design Pressure (barg) (internal/external)	Design Temperature (°C)	Ultimate Strength (MPa)	Yield Strength (MPa)	Allowable Stress (MPa)	Young's Modulus (GPa)	Poisson's ratio, ν
Bottom section	15Mo3	1.67/1.0125	405	440	150	100	181	0.3
Top section (old)	HII	1.67/1.0125	350	410	140	93.3	187	0.3
Top section (new)	BS 1501-151-430B	1.67/1.0125	350	430	140	102	187	0.3

Element type definition

Since the pressure vessel is axis symmetrical, and the loads are applied in all three dimensions, it is necessary to select an appropriate element for this shell, i.e. SHELL281. This is an eight-node element suitable for thin to moderately thick structures.

Meshing

This is another key step during the modelling process which allows for refinement in element size once the basic geometry of the model has been developed. Furthermore, mesh refinement allows for an accurate prediction of the stresses within the elements.

Boundary conditions

The application of boundary conditions will mainly depend on the type of assessment, for example, when assessing the structure for plastic collapse, the boundary conditions are going to be internal pressure, weight and displacement. On the other hand, when assessing for buckling, the boundary conditions will be external pressure, weight, wind loads and displacement.

Maintenance Engineering

There are two types of maintenance, breakdown or reactive maintenance and preventive maintenance. The other type of maintenance is corrective maintenance, which is more of a subset to preventive maintenance rather than a standalone maintenance system. The main difference between these maintenance types is that the former is implemented once a piece of machinery fails to function whilst the latter provides for maintenance tasks that are implemented to prevent a machinery from failing to perform its intended function.

Breakdown/Reactive maintenance

There are advantages and disadvantages related to this maintenance program. Some of the advantages are equipment failure has no significant impact to the overall operation of a plant. This may be true when there is sufficient redundancy in the system where such a failure of a component/machine instantly activates a standby machine to continue with the operation. Furthermore, it may be a related to costs whereby a return in investment is much greater by running a particular component/machine to failure.

However, there are also disadvantages related to this maintenance program. One of the disadvantage could be the high cost related to a sudden failure of a component/machine resulting to extended outages and lead times to repair damaged components/machines. The other disadvantage is that there

is little to no investigation that is conducted to accurately analyse the cause of the failure of that machine. The danger is that there could be repetitive failures in the future that may go unnoticed and subsequently affect the operation profits.

Preventive maintenance

This is a more structured systematic approach maintenance program. It may be costly exercise if the early development work to establish the need of such a program is not properly analysed such that the cost to implement is much lower than the cost to repair critical equipment during breakdown maintenance. This type of maintenance program consists of three sub-tasks [11]:

a) Predictive maintenance

   The service life of important parts is predicted based on inspection or diagnosis, in order to use the parts to the limit of their service life in this method. Compared to periodic maintenance, predictive maintenance is condition-based maintenance. It manages trend values, by measuring and analyzing data about deterioration and employs a surveillance system, designed to monitor conditions through an on-line system. Some of the common techniques associated with predictive maintenance are vibration monitoring, oil analysis, visual inspections, thermography, operating window monitoring and non-destructive testing.

b) Periodic maintenance

   Time based maintenance consists of periodically inspecting, servicing and cleaning equipment and replacing parts to prevent sudden failure and process problems.

c) Corrective maintenance

   It improves equipment and its components so that preventive maintenance can be carried out reliably. Equipment with design weakness must be redesigned to improve reliability or improving maintainability. The main benefit of corrective maintenance is that equipment overhaul is planned thoroughly and the related labour requirements to repair damaged components. This allows for optimal budget allocations and maximise plant availability.

High vacuum column maintenance strategy

The high vacuum column is categorised as a pressure vessel and as such regulated by the PER concerning legal requirements for inspections. The PER specifies periodic maintenance (statutory inspections) interval of 3 years which may be extended to maximum 9 years provided a dispensation is in place or the site has an approved RBI system. It is worth noting that the current inspection interval of the vacuum tower is 6 years. The other maintenance program applicable to the high vacuum column are predictive maintenance in the form of visual inspections, non-destructive testing and operating window monitoring. The actual inspection intervals associated with the high vacuum column are aligned to unit turnarounds where a major scope of periodic maintenance is undertaken to minimise unit breakdowns.

CRITERIA FOR VALIDATION

The criteria for validation of the results is specified in API 579 annexure B [9], depending on the type of failure each load case induces on the vacuum tower. Five failure modes are outlined that need to be satisfied to qualify components for future operation. These failure modes are [9]:

1. Protection against plastic collapse

   In the evaluation of a component for plastic collapse, equivalent stress values are calculated based on stress categories, i.e. general primary membrane equivalent stress (P_m), local primary membrane equivalent stress (P_L) or primary membrane plus bending equivalent stress (P_L+P_b). These calculated equivalent stresses are then compared to the allowable stresses as shown on Figure 11 below.

   Based on the stress categories already defined above, the loads applicable in this evaluation are internal design pressure and other mechanical loads such as wind.

2. Protection against local failure

   This evaluation focuses more on the localised thinned regions over and above plastic collapse in which an algebraic sum of the linearized principal stresses is evaluated and then compared to four times the allowable stress of the material. Loads applied are the same as those under plastic collapse.

3. Protection against collapse from buckling

   In the evaluation of a component for buckling, bifurcation analysis is performed on the structure using elastic stress analysis in which a minimum design factor of 2.5 is established. The applicable loads for buckling evaluation are external pressure and axial compression.

4. Protection against failure from cyclic loading

   In this assessment, a component is assessed for fatigue to determine if the allowed cycles are not exceeded by the number of unit startup/shutdown, pressure/temperature variations, and thermal

stresses during its operation. Based on the loading history and operation of the high vacuum column, it is not under cyclic loading.

5. Protection against creep or creep-fatigue damage

In this assessment, historical operating data is required to determine if the component's material microstructure properties are affected and whether any creep damage occurs which result in complete depletion of the component's mechanical properties. Based on the material properties of the high vacuum column, creep is not considered since the design temperature is below the creep range.

Stress Category	Primary			Secondary Membrane plus Bending	Peak
	General Membrane	Local Membrane	Bending		
Description (For examples, see Table 5.2)	Average primary stress across solid section. Excludes discontinuities and concentrations. Produced only by mechanical loads.	Average stress across any solid section. Considers discontinuities but not concentrations. Produced only by mechanical loads.	Component of primary stress proportional to distance from centroid of solid section. Excludes discontinuities and concentrations. Produced only by mechanical loads.	Self-equilibrating stress necessary to satisfy continuity of structure. Occurs at structural discontinuities. Can be caused by mechanical load or by differential thermal expansion. Excludes local stress concentrations.	1. Increment added to primary or secondary stress by a concentration (notch). 2. Certain thermal stresses which may cause fatigue but not distortion of vessel shape.
Symbol	P_m	P_L	P_b	Q	F

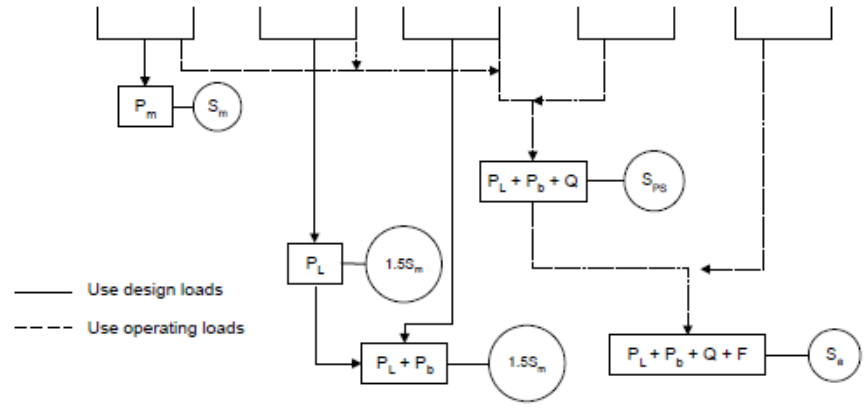

Figure B1.1
Stress Categories and Limits of Equivalent Stress

Figure 11 Stress category limits for plastic collapse analysis [9]

DESIGN BY ANALYSIS (LEVEL 2)

Plastic Collapse

Table 2 Plastic collapse applied loads

Load type	*Magnitude*
Internal pressure	167 kPa
Weight of structure above thinned area	120000 kg
Wind force	88150 N

Applicable loads

The applicable loads for plastic collapse are shown on Table 2 above. Internal pressure and weight have been obtained from the data sheet of the high vacuum column. The total operating weight of the vacuum column is 356000kg, it was assumed that 2/3 of the weight acts on the bottom section and that 1/3 of the weight acts on the top section of the column. See appendix 1 for the detailed calculation to establish the wind force per SANS 10160-1.

A first principle assessment was performed to determine the stresses on the thinned section due to the applied loads as indicated on Table 2. The detailed calculations are shown on Appendix 2, and the results are as follows:
The maximum membrane stress due to these loads is 82.6 MPa and the minimum thickness required at this membrane stress is equal to 6.7mm. Both these values are acceptable since the allowable stress is 93.3 MPa and the minimum measured thickness is 7.6mm.

Buckling

All loads resulting to a buckling failure are shown on Table 3 due to external pressure and Table 4 due to axial stresses. In buckling analysis, a structure is assessed for structural stability under a compressive stress field. This analysis consists of assessing stability due to axial compression and also due to application of external pressure (vacuum condition).

Applicable loads

Table 3 Buckling loads, external pressure assessment

Load type	*Magnitude*
External pressure	101.325 kPa
Weight of structure due to gravity	9.81 m/s2
Wind shear force	88150 N

Table 4 Buckling loads, axial stresses assessment

Load type	*Magnitude*
Total weight of structure	3.492E6 N
Weight of structure due to gravity	9.81 m/s2
Wind shear force	88150 N

External pressure

A first principle assessment was conducted to determine effect of external pressure, detailed assessment in Appendix 3 (1) and the results are:

Maximum allowable external pressure is 20 kPa, this is far less than the applied external pressure which therefore means the structure is not safe for operation under full vacuum conditions. This assessment is regarded as a level 2 assessment in API 579. The only other assessment that can be done a level 3 assessment (FEM) before a decision is made with regards to continued safe operation of the vessel.

Combined loads

The other load case that has to be satisfied for buckling analysis is the effect of axial compression. A first principle assessment is conducted and detailed results are in Appendix 3 in which two conditions have to be satisfied:

$10.5 \leq 1.0, fail\ for\ \lambda_c \leq 0.15$, axial compression, compression bending, shear and hoop compression, and

$0.33364 \leq 1.0, pass\ for\ \lambda_c \leq 0.15$, axial compression, compressive bending and shear

From the above results, the structure fails the analysis for combined loading.

Additional stiffening ring

One of the possible solutions would be add a new stiffening ring so that a level 2 assessment can yield positive results. This ring has been added about halfway on the thinned section, i.e. 650mm above the bottom ring located at 11610mm elevation. The figure below shows location of a new ring. Design by analysis results as indicated in Appendix 4 show that by adding a new ring the level 2 assessment for external pressure is acceptable, i.e. maximum allowable pressure is 108kPa. However, the level 2 assessment results from axial compression are still not satisfactory:

$1.75 \leq 1.0, fail\ for\ \lambda_c \leq 0.15$, axial compression, compression bending, shear and hoop compression, and

$0.33364 \leq 1.0, pass\ for\ \lambda_c \leq 0.15$, axial compression, compressive bending and shear

From the above results, the structure fails the analysis for combined loading.

Even though the level 2 assessment fails under combined loadings, the margin is significantly less when compared to the assessment without an additional ring. The next natural step is to check the effect of the additional ring on the level 3 (FEM) assessment.

FEM MODELS (LEVEL 3)

Plastic Collapse

Applicable loads

The applicable loads for plastic collapse are shown on Table 2 above. Internal pressure and weight have been obtained from the data sheet of the high vacuum column. The total operating weight of the vacuum column is 356000kg, it was assumed that 2/3 of the weight acts on the bottom section and that 1/3 of the weight acts on the top section of the column. See appendix 1 for the detailed calculation to establish the wind force per SANS 10160-1.

Due to symmetry, half the model has been modelled in Ansys, using Ansys Workbench. Material properties at the design temperature have been specified on the model per Table 1. Geometry developed in Design Modeler with a varying thickness applied on the thinned section to simulate effect of corrosion. Mesh of 5mm was applied onto the 2D model as shown below.

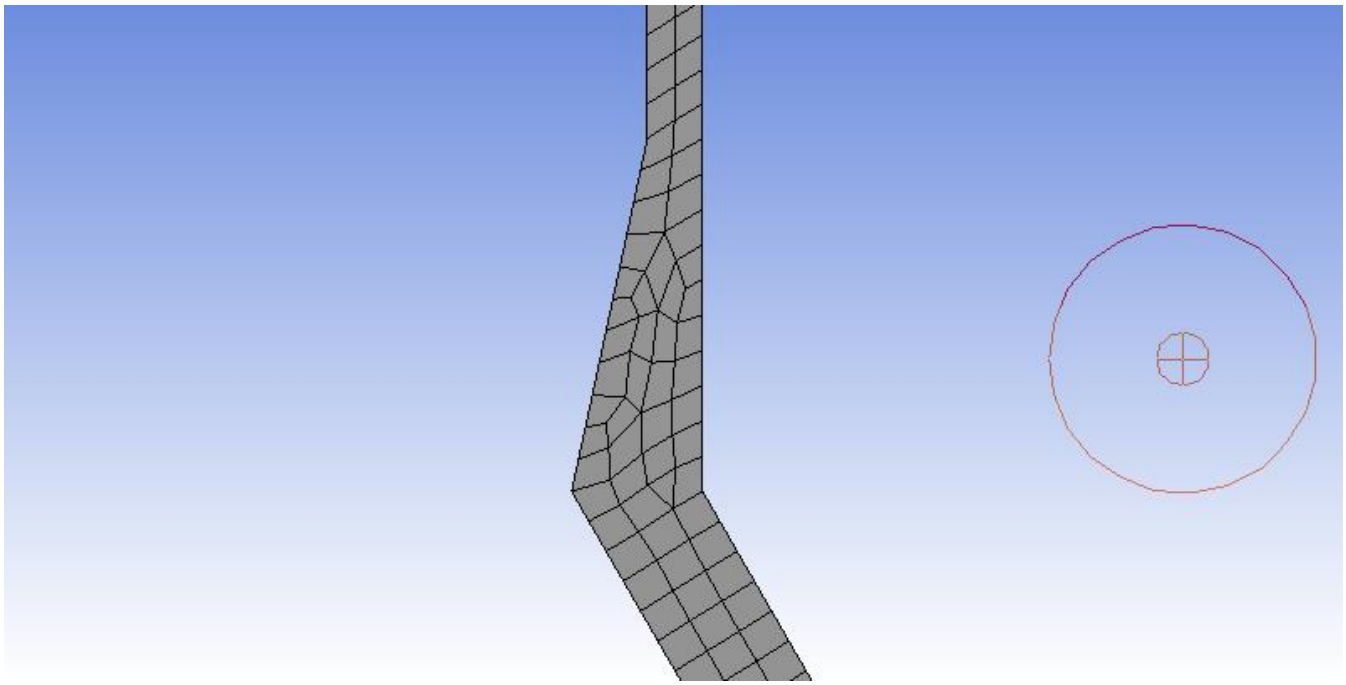

Figure 12 Mesh above conical section

Internal pressure was applied on the inside edge of the model, weight on the top edge in the negative y-direction and wind force on the top edge along the x-axis to simulate bending moments.

Local failure

This analysis establishes whether local failure due to strain limits is acceptable on the component under investigation. There are two methods that may be used to qualify component for local failure:

- Elastic analysis, and
- Elastic-plastic analysis

Buckling

External pressure

A complete 3D model of the high vacuum column was modelled in Ansys with a thickness of varying degree as shown on Table 5 below,

Table 5 Thickness profile of the high vacuum column

Location	*Material of construction*	*Thickness (mm)*
Bottom dished head	15Mo3	21
Bottom shell section	15Mo3	19
Conical section	15Mo3	19
Top section, thinned section	HII	7.6
Top section, above thinned section	BS 1501-151-430B	16
Skirt	15Mo3	16

Figure 13 depicts the full 3D model with the stiffening rings on the shell sections.

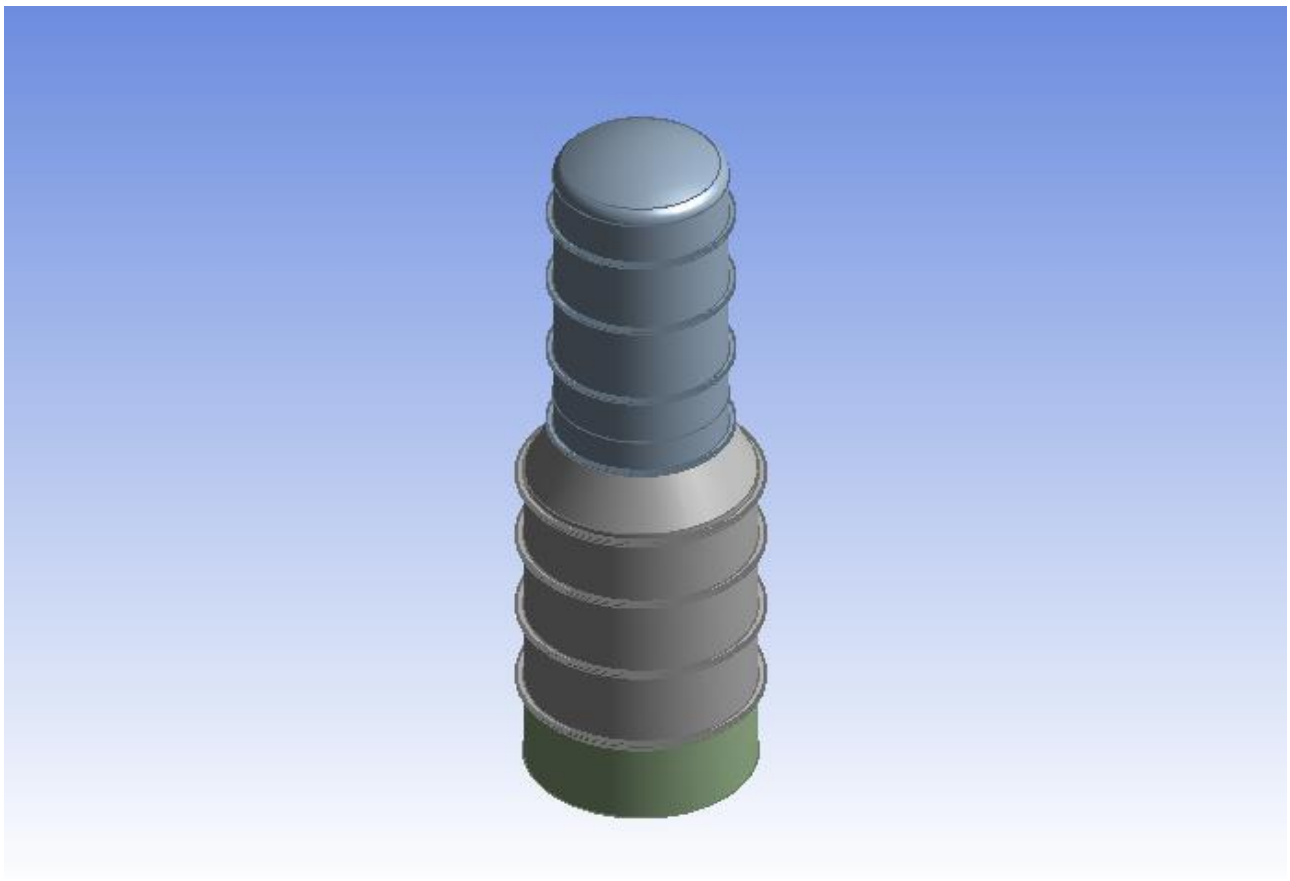

Figure 13 High vacuum column 3D model

The entire bottom section is cladded with a stainless steel liner, hence no corrosion removed, but the top section is not lined and therefore in the assessment a corrosion allowance of 3mm was removed from the nominal thickness.

For external pressure, the allowable design factor is 2.5 per API 579 Annex B1.4.1. A linear bifurcation analysis was conducted to determine the buckling load factors under the loads specified in Table 3.

A full body mesh was applied on the model, using element size of 200mm. A close up of the meshed surface is shown on Figure 14. For the mesh a SHELL281 element was specified with a target mesh quality of 0.05 producing 299310 elements from 107632 nodes.

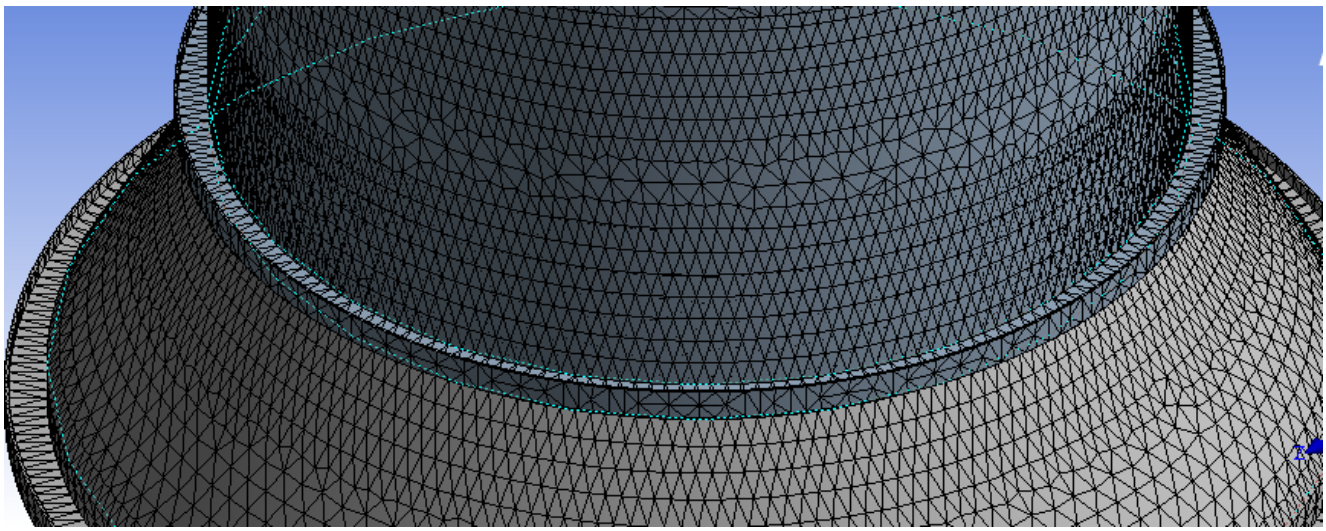

Figure 14 Meshed region, bottom to top section

Finite element modelling, combined loads

An Ansys model was developed with the loads on Table 4 applied to the high vacuum column. The model geometry and meshing is the same as for the external pressure case except for the applied loads. For axial compression, the allowable design factor is 7.3 per API 579 Annex B1.4.1. A linear bifurcation analysis was conducted to determine the buckling load factors under the loads specified in Table 4. Applied loads are shown on Figure 15 below in which 2/3 of the weight is specified on the bottom section and 1/3 of the remaining weight on the top section, total operating column weight is 356000kg.

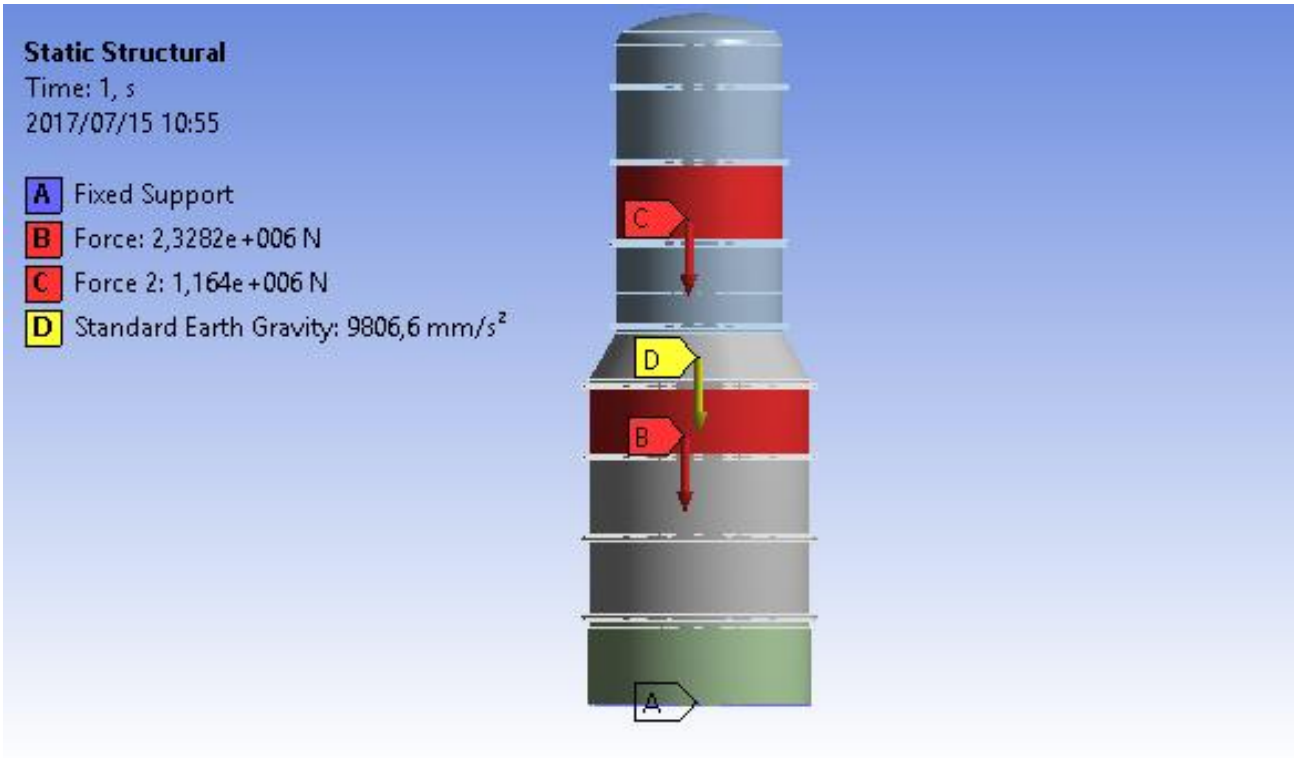

Figure 15 Applied loads for buckling axial compression

Additional stiffening ring

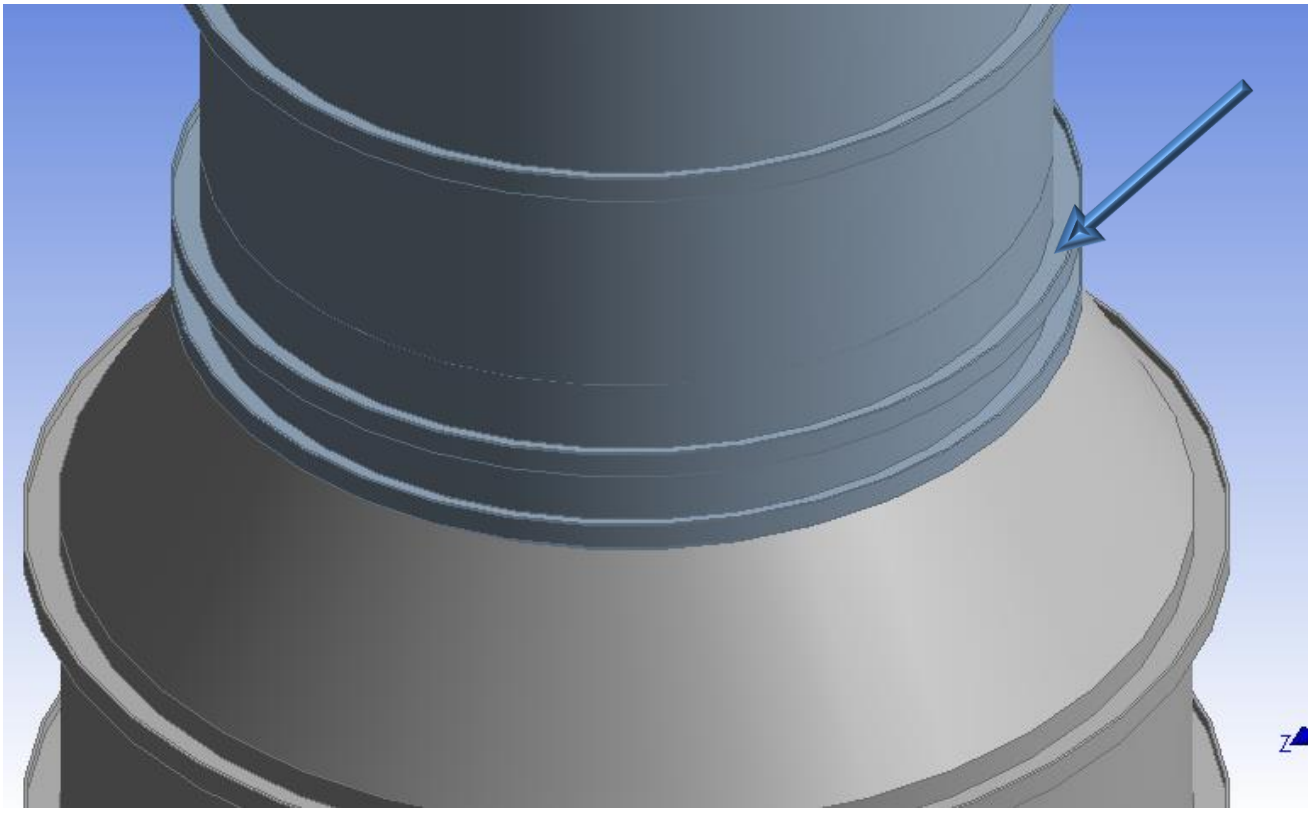

Figure 16 Location of new stiffening ring

FEM RESULTS

Protection against plastic collapse

Ansys model results

The maximum equivalent (von-Mises) stress under the loads specified is 88MPa as shown on Figure 17.

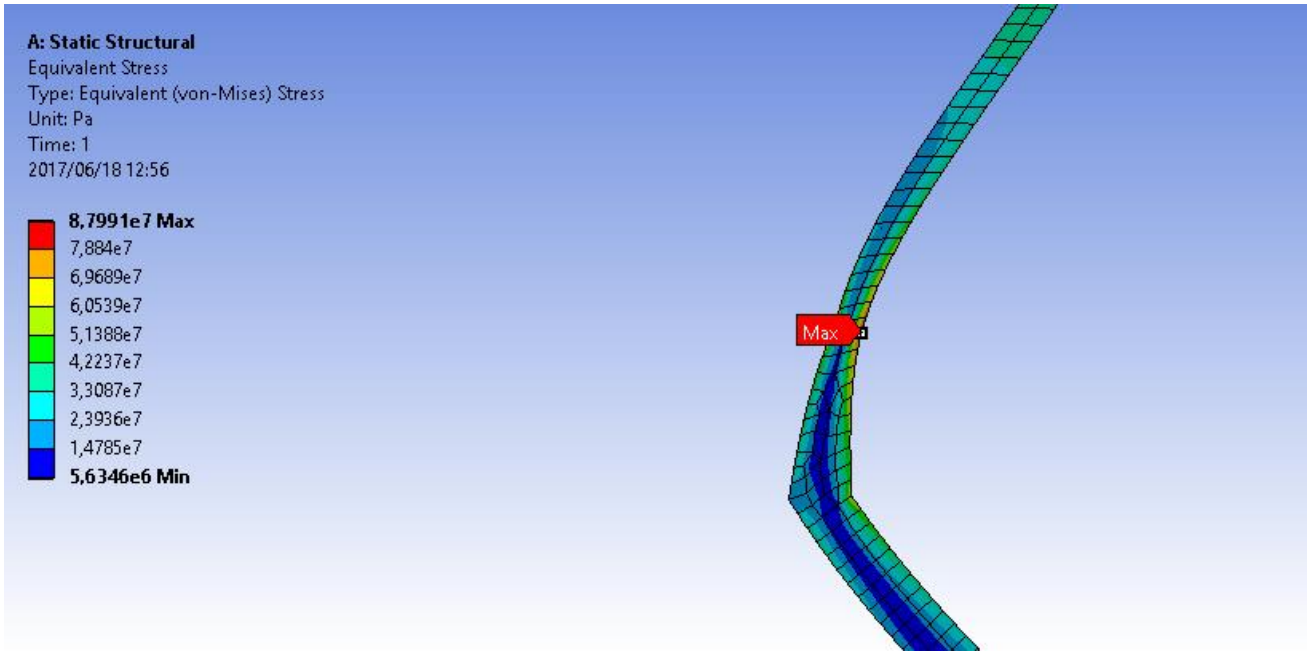

Figure 17 Plastic Collapse Equivalent Stress

In order to verify acceptance for plastic collapse under the specified loads, various linearized stresses have to be established.

Table 6 Stress classification lines (SCL) results summary

SCL no	Location	Material	Sm	Linearized Stresses			Acceptance Criteria		
				Pm	PL	Pb	Pm≤Sm	PL≤1.5Sm	Pl+Pb≤1.5Sm
1	Bottom shell (away from discontinuities)	15Mo3	100	35.3	N/A	N/A	ok	N/A	N/A
2	Bottom shell to cone junction	15Mo3	100	N/A	14.695	N/A	N/A	ok	N/A
3	Top shell to cone junction	HII	93.3	N/A	8.7335	N/A	N/A	ok	N/A

4	Top section (near discontinuities)	HII	93.3	N/A	16.195	N/A	N/A	ok	N/A
5	Top corroded section	HII	93.3	73.3	N/A	N/A	ok	N/A	N/A
6	Top section (away from discontinuities)	BS 1501-151-430B	102	36.65	N/A	N/A	ok	N/A	N/A

A depiction of the linearized stresses is shown below for each of the stress classification line.

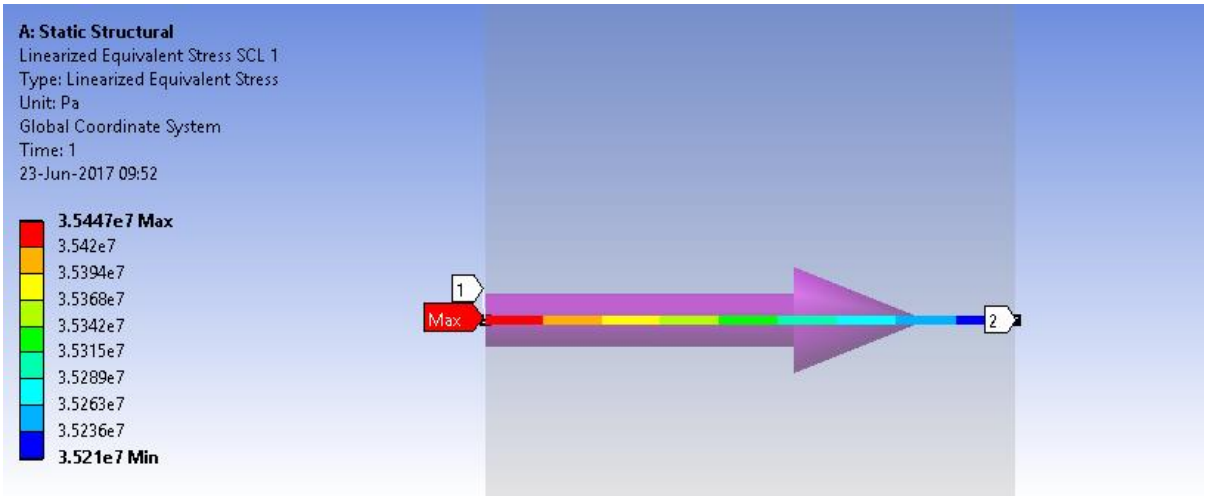

Figure 18A SCL 1 stresses

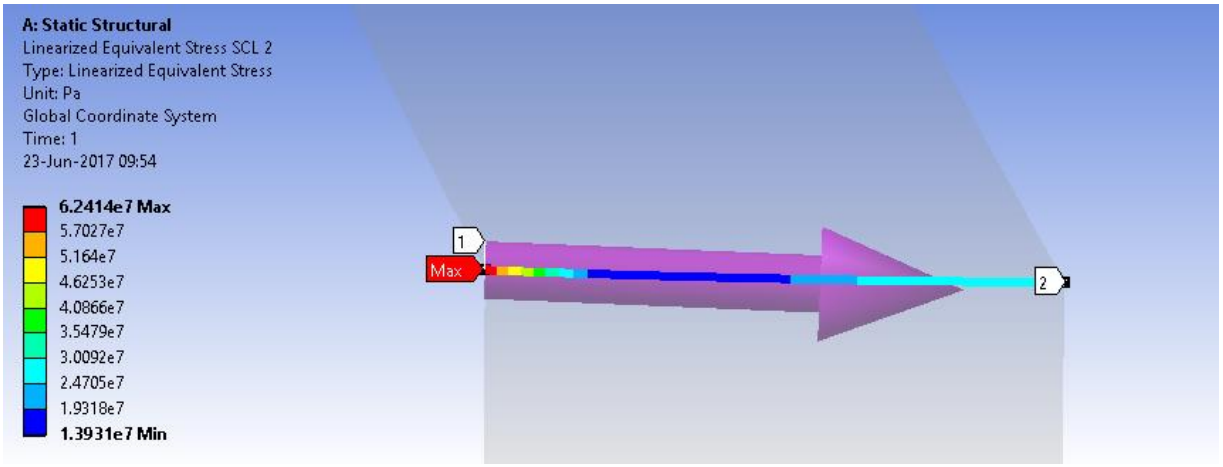

Figure 18B SCL 2 stresses

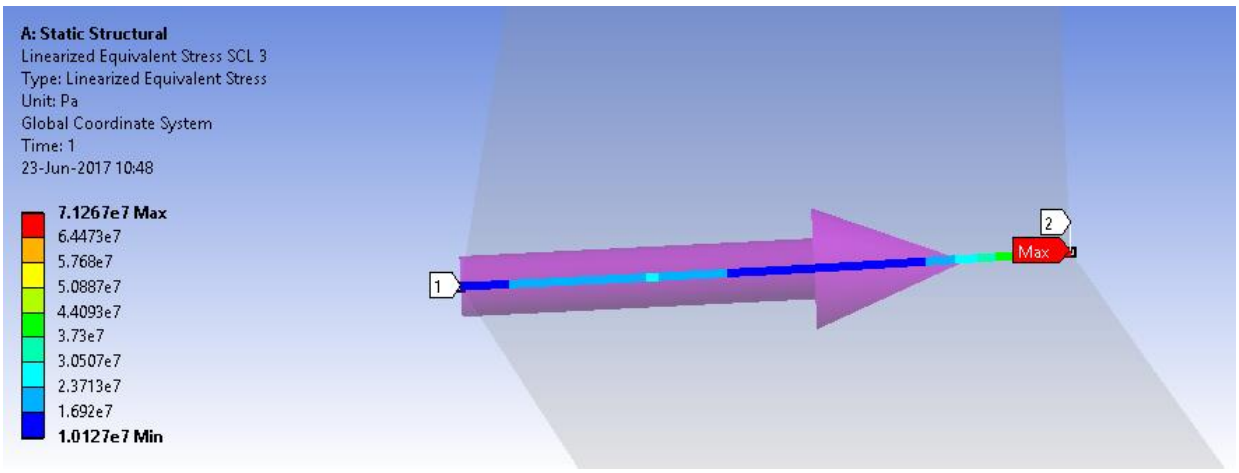

Figure 18C SCL 3 stresses

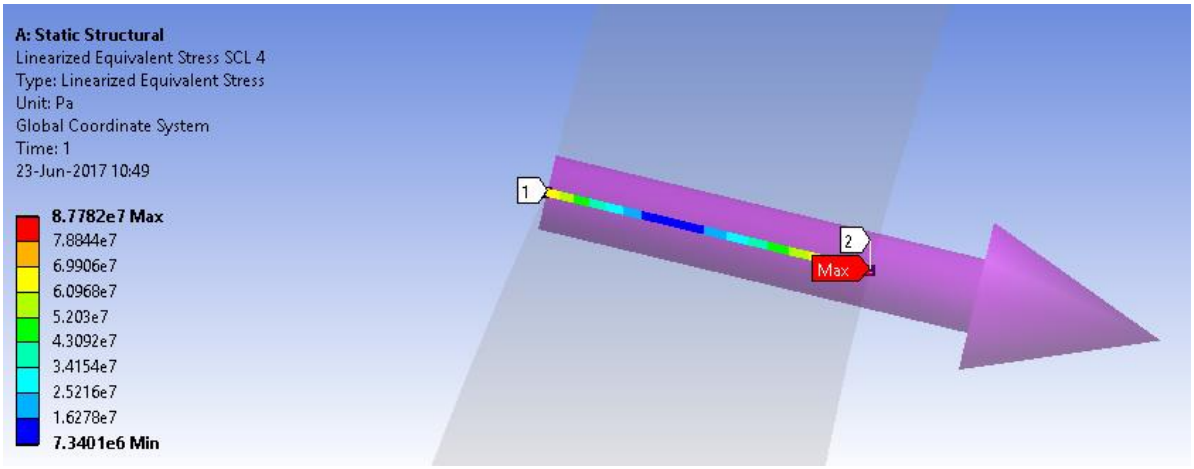

Figure 18D SCL 4 stresses

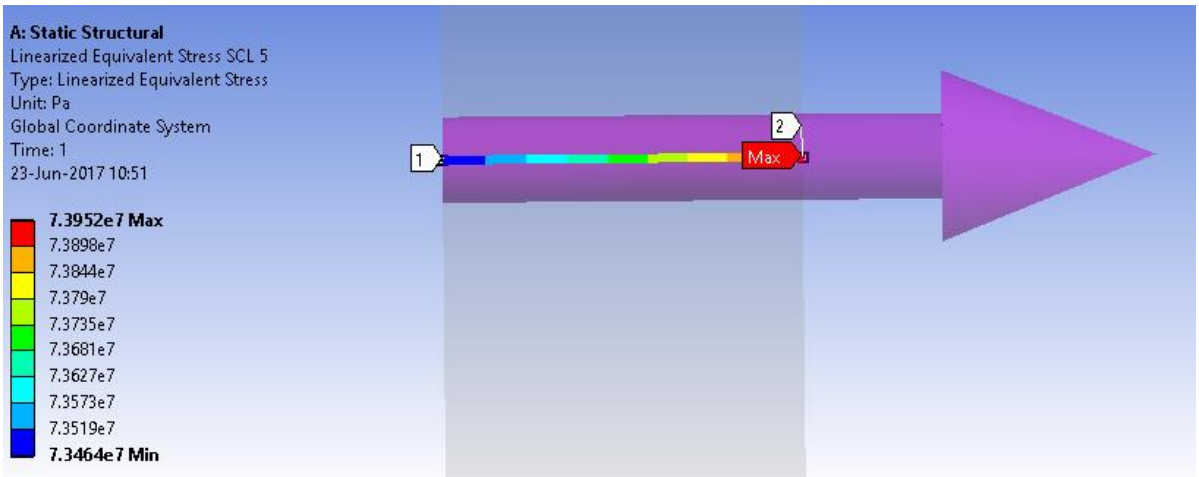

Figure 18E SCL 5 stresses

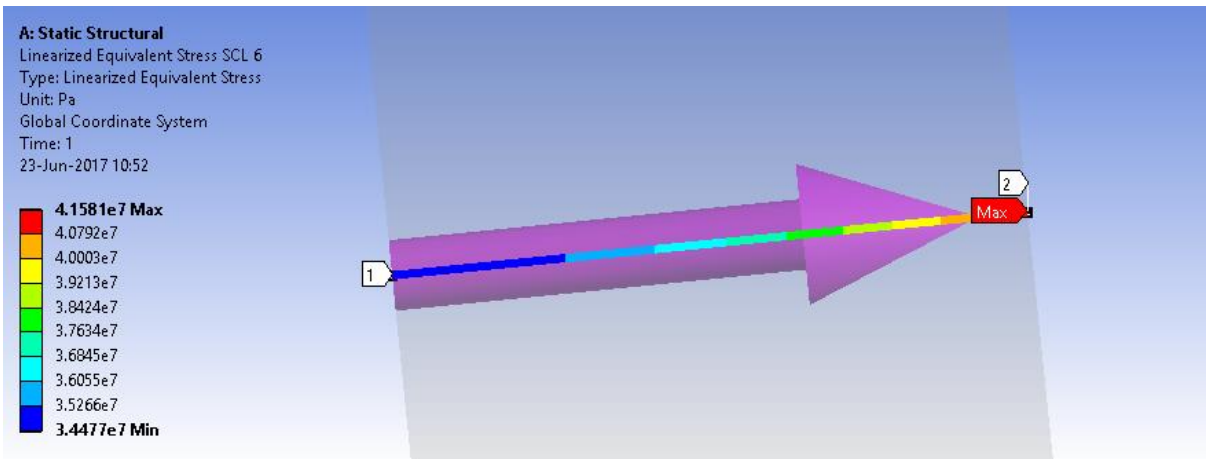

Figure 18F SCL 6 stresses

Protection against local failure

In order to satisfy requirements for local failure, the sum of the principal stresses must be less than or equal to four times the allowable stress when evaluating using the elastic analysis.

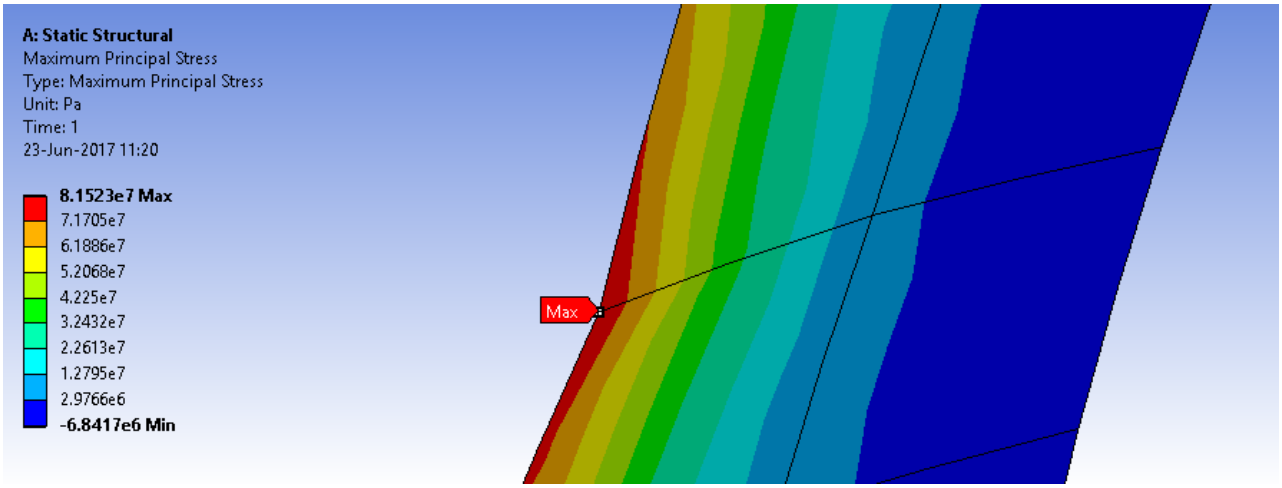

Figure 19 Local failure elastic analysis results

The maximum value of the sum of principal stresses as shown on Figure 19 is 81.523MPa. the following has to be satisfied:

$81.523 \leq 4 \times S_m \leq 4 \times 93.3 \leq 373.2$ [9]

From the above assessment, local failure is not possible at the applied loads and thicknesses.

Protection against failure from buckling

A linear static analysis is only required before a buckling analysis is performed. Results of the buckling analysis are shown in Figure 20.

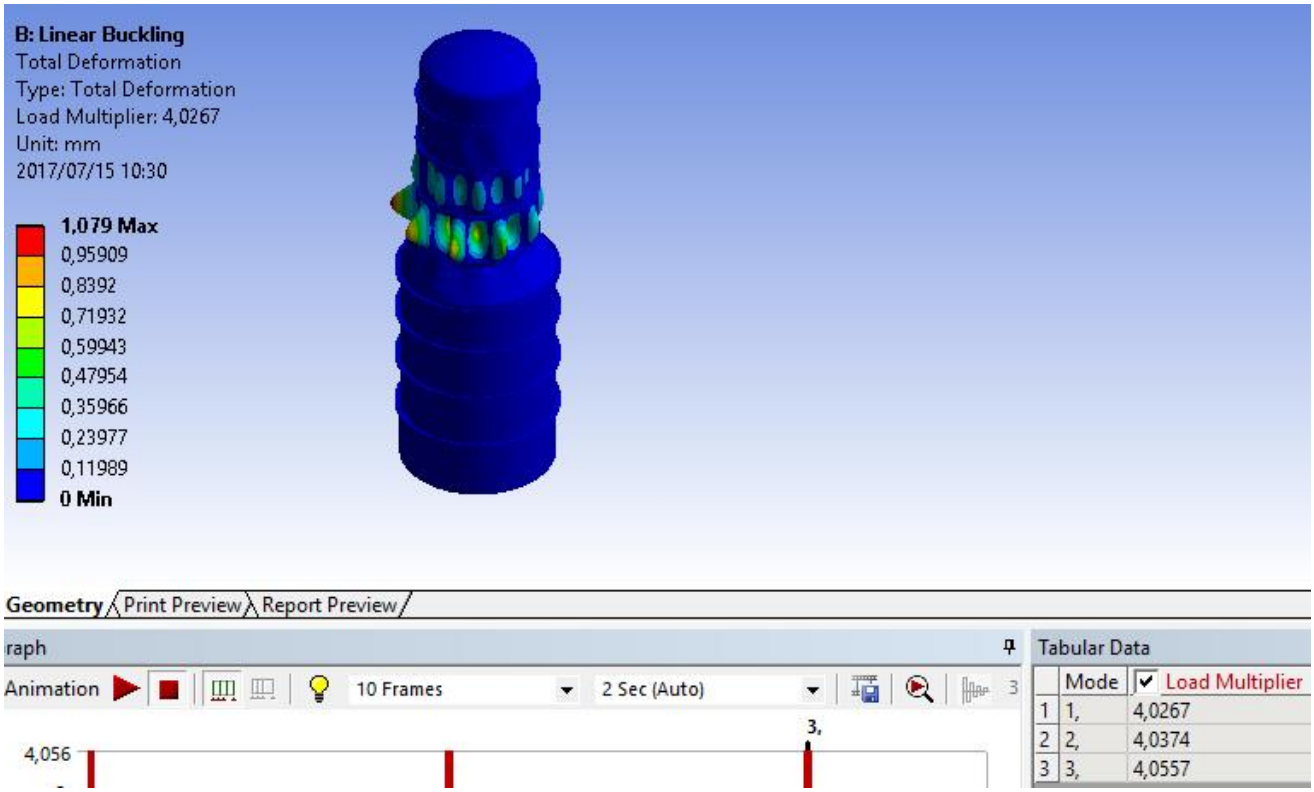

Figure 20 Linear buckling results, external pressure

The design factor, minimum, at the current wall thickness and external pressure is 4.0267 which is greater than 2.5. This is deemed a level 3 assessment per API 579.

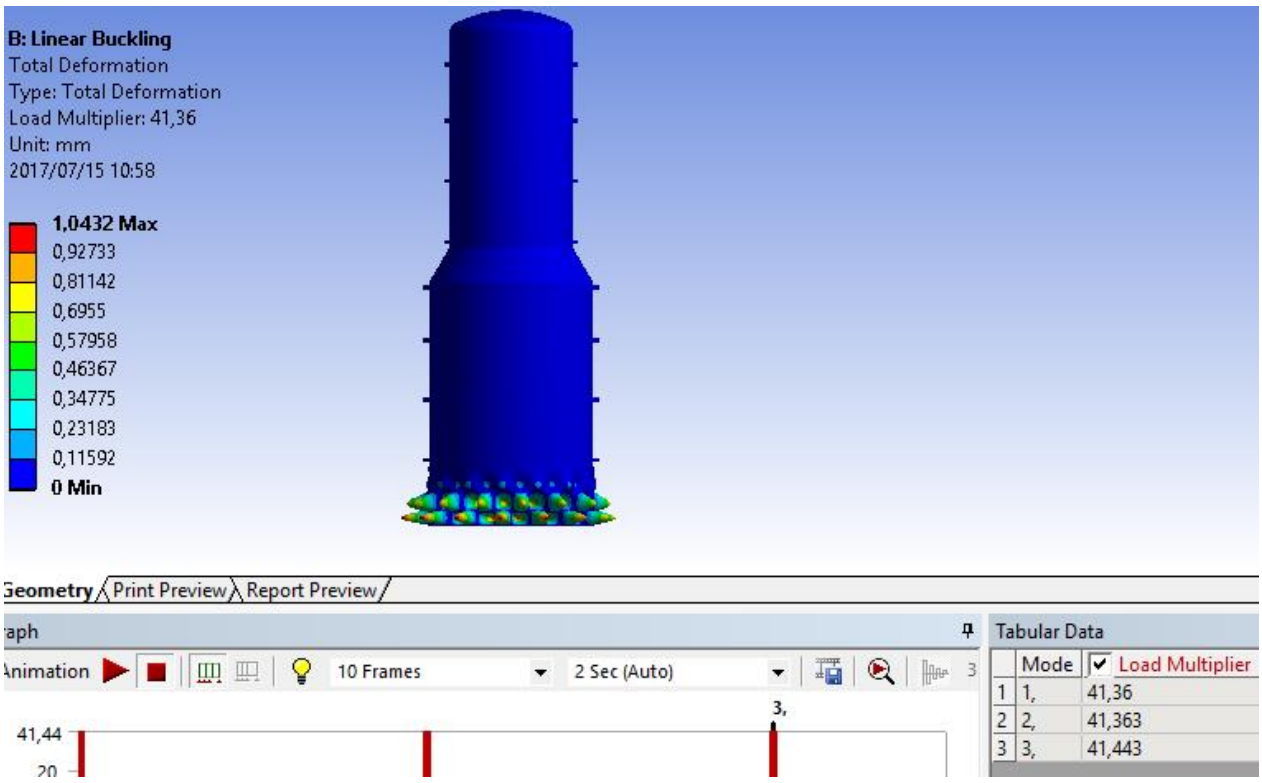

Figure 21 Linear buckling results, axial compression

The design factor, minimum, at the current wall thickness and external pressure is 41.36 which is greater than 7.3. This is deemed a level 3 assessment per API 579.

The FEM results for external pressure is shown in Figure 22, with the additional ring. All boundary conditions, meshing remain the same but the only change is that a new additional ring has been added onto the model.

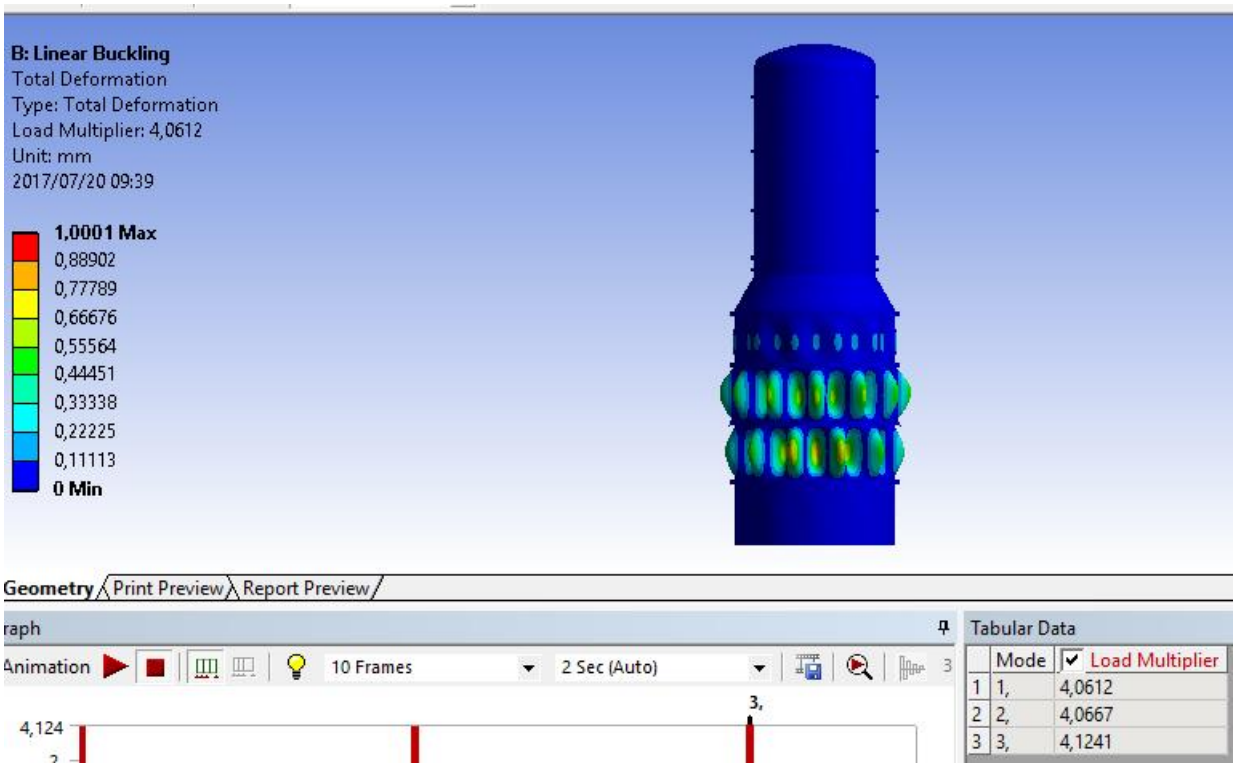

Figure 22 FEM results with additional ring, external pressure

The results indicate a shift in buckling location due to the stiffening effect on the thinned section. The visuals indicate buckling on the bottom section with a buckling load factor of 4.0612 which is still well above the design factor of 2.5 based on external pressure.

For combined loading, the results do not change that much.

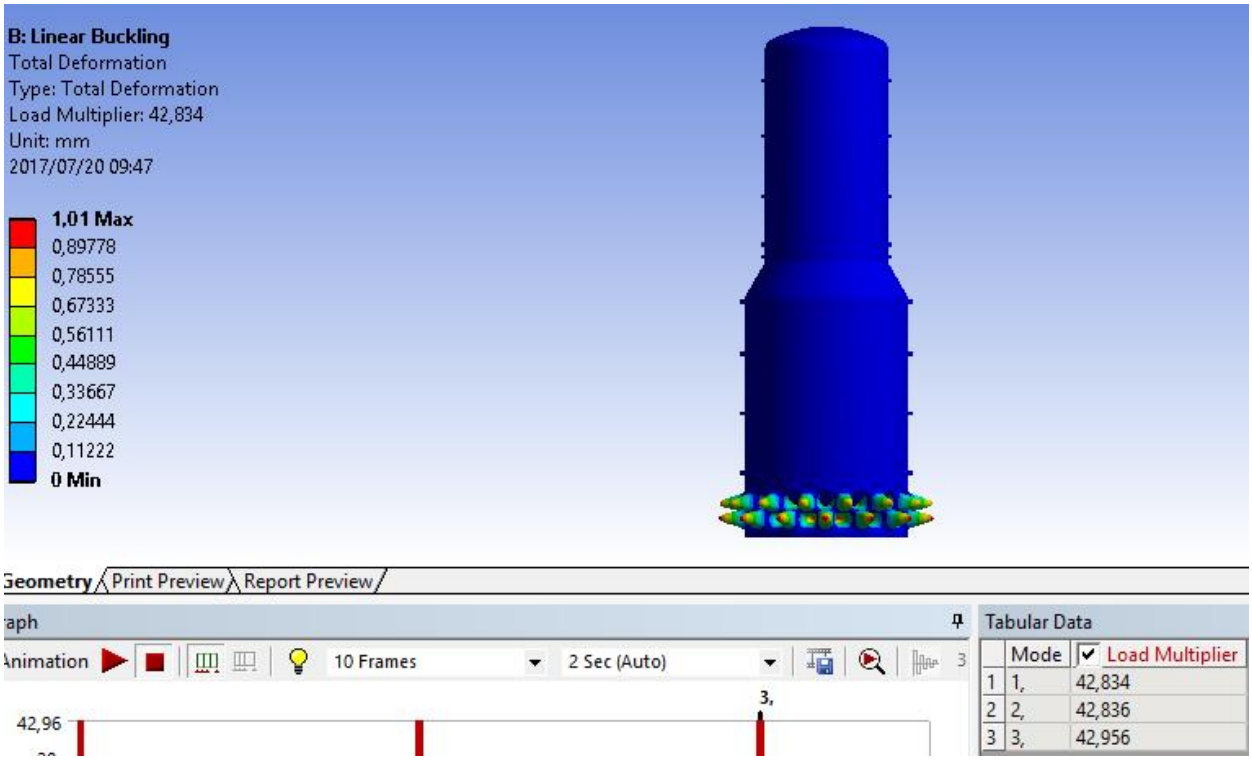

Figure 23 FEM results with additional ring, combined loads

There is slight increase in the buckling load factor as indicated on Figure 23, i.e. new buckling load factor becomes 42.834 and the design factor remains the same at 7.3. these results confirm that the structure is safe based on a level 3 assessment under combined loading.

DISCUSSION

FEM results

The results from the finite element analysis deduce that internal and axial compression loads are not determining load cases for failure but rather buckling is the most prevalent failure mode under external pressure. The stresses due to internal pressure at the thinned section are well within the allowable limits, this has been confirmed by hand calculations on the appendices. There is a limit however, this is based on the minimum thickness required for internal pressure, this limit is 6.7mm. Thickness values below this limit will render the high vacuum column unsafe due to the exceedance of membrane stress limits from the material of construction.

At the various shell section of the high vacuum column, linearized stresses were developed in order to ensure compliance to the stress classifications. None of the stress categories were exceeded at the current thickness of 7.6mm. there is a very small margin of future corrosion before the limits apply, i.e. difference from 7.6mm to 6.7mm. on this basis, the high vacuum column is protected from plastic collapse failure.

Protection against failure from bucking is twofold, one from external pressure only and the other from combined loads resulting onto axial compression. In the first instance, the high vacuum column fails the level 2 assessment as the limit in pressure is much less than the actual operating pressure under full vacuum conditions, i.e. -101.325kPa. A level 3 assessment was conducted at the current thickness of 7.6mm, this involved performing finite element modelling using Ansys computer software. The buckling load factors from the model are higher than design factors, hence buckling failure due to external pressure is not possible.

In the second instance, the high vacuum column fails the level 2 assessment for combined loading since the calculated combined stresses (axial compression, compression bending, shear and hoop compression) are not less than unity. A level 3 assessment was conducted at the current thickness of 7.6mm, this involved performing finite element modelling using Ansys computer software. The buckling load factors from the model are much higher than the design factors, hence buckling failure due to combined loading is not possible. A further assessment was performed to check the effect of an additional stiffening ring. This does not help much as the final results do not change that much. It does however, move the effect of buckling due to external pressure to the bottom section rather than the thinned section under review.

It is evident from the inspection data that even though the high vacuum column is deemed safe now, it is imperative that a study is conducted to properly assign inspection intervals together with the relevant scope of inspection. This goes beyond the high vacuum column as other system in the same operation regime need to be reviewed based on this high corrosion rate established. The corrosion rate as already noted is about 0.3mm per year. This therefore means that the remaining life of the high vacuum column is approximately a year and a half from the date of inspection which was June 2015.

Remaining life assessment

The high vacuum column suffers from Naphthenic Acid Corrosion (NAC). This is confirmed per API 571 damage mechanisms. The mechanism has been discussed in detail under the literature review. Operating temperatures on the thinned region are normally in a range of 230-276 ℃ as shown on figure 24.

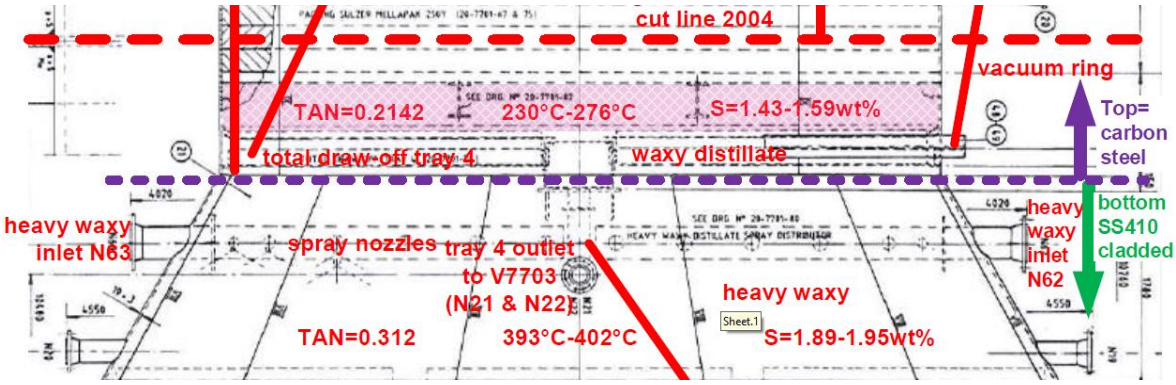

Figure 24 Temperature profile on the high vacuum column

As defined in API 571, NAC normally occurs at temperatures of about 218 ℃ and increases in severity up to 400℃, the region under assessment is well within the NAC attack envelope.

Design minimum thickness

In general, pressure equipment design thickness governs the replacement or repair of such equipment, only in special cases where detailed fitness for service assessments are carried out to render equipment safe for continued operation. The calculated minimum thickness for the thinned section is 6.7mm for internal pressure per Appendix 2 or 15mm for external pressure per Appendix

5, whichever is greater. Therefore, the design thickness for the thinned section excluding corrosion allowance is 15mm.

Corrosion rates

In API 510 [12], the calculation for corrosion may be based on long term corrosion rate or short-term corrosion rate, the latter relies on mainly good historical inspection data. To be conservative, the calculation will be based on a long-term basis:

$$Corrosion\ rate\ (LT) = \frac{t_{initial} - t_{actual}}{time\ between\ t_{initial} and\ t_{actual} (years)} = \frac{19 - 7.6}{39} = 0.3mm/year$$

The thinned section has no corrosion protection, but it has a corrosion allowance of 3mm. An estimate of the high vacuum life can be established from this information.

The calculated life of the thinned section becomes 10 years based on this corrosion rate.

Generally, pressure vessels are designed for minimum 20-year life, in this case, the corrosion rate is significantly higher than normal and therefore some form of corrosion protection should have been implemented. The high vacuum tower inspection interval is currently on the 6-year interval, this is not sufficient at the current corrosion rate.

Reliable maintenance plan proposal

It is proposed that a predictive maintenance strategy is adopted for future inspections other than the current periodic maintenance strategy for the following reasons:

- ***On-stream inspections***

  This allows for corrosion monitoring and confirmation of the calculated long-term corrosion rates. A frequency not more than three months shall be set to accurately predict the remaining life.

- ***Crude selection***

  The aggressiveness of naphthenic acid corrosion relies mainly on the type of crude oil that is being processed by the plant. Crudes containing low sulphur must be avoided since they cannot provide for a protective iron sulphide which forms a barrier from attack due to naphthenic acids. It is a known factor that some of the low sulphur crudes have an economic benefit but should not be the case at the expense of safety.

CONCLUSIONS

The use of high level finite element modelling has proven to be a useful tool in confirming safe operation of the high vacuum columns under corrosion where first principle approach has become limited. This confirms one the main benefits of finite element modelling, costs of unplanned outages can be averted. The various models developed are a useful tool for future use on similar equipment to ensure failure can be safely predicted. These models included loads such as internal pressure, external pressure and structural loads.

Due to the significant corrosion on the high vacuum column, it is not possible to defer a permanent repair any longer. Therefore, within a year a repair must be formalised, this may take the form of weld building up the thinned section with carbon steel up to nominal thickness and then cladding the section with 400 series stainless steel. Alternatively, a new canned section must be installed to replace the thinned top section. Based on the on-stream inspection data, a new inspection interval must be put in place to ensure that any future corrosion attacks are detected early and prevention measures put in place.

RECOMMENDATIONS FOR FUTURE WORK

- Conduct on-stream inspections to accurately predict corrosion rates based on selected crude diets
- Selection of resistant materials to naphthenic acid attack such as low alloy steel with Molybdenum or 300 series stainless steels
- Fully assess existing circuits that may be under corrosion attack and clad carbon steel sections with 400 series stainless steels

REFERENCES

1. Fahim, M.A., Al-Sahhaf, T.A., Elkilani, A.S. (2010). *Fundamentals of Petroleum Refining*. Great Britain: Elsevier.
2. Moss, D. (2004). *Pressure Vessel Design Manual*. United States of America: Gulf Professional Publishing.
3. NACE International (2000). *Basic Corrosion CD-ROM Study Manual*.
4. Stensbury, E.E., Buchanan, R.A. (2000). *Fundamentals of Electrochemical Corrosion*. United States of America: ASM International.
5. American Petroleum Institute (API) (2011). *Damage Mechanisms Affecting Fixed Equipment in the Refinery Industry, API 571, 2nd Edition.* Washington: API Publishing Services.
6. Jones, R.H. (1992). *Stress-corrosion cracking Materials Performance and Evaluation*. United States of America: ASM International.
7. Juvinall, R.C., Marshek, K.M., (2000). *Fundamentals of Machine Component Design*. United States of America: John Wiley & Sons, Inc.
8. Pao, P.S. (1991). Mechanisms of Corrosion Fatigue. *Fatigue and Fracture volume 19.*
9. American Petroleum Institute (API) (2007). *Fitness for Service, API 579, 2nd Edition.* Washington: API Publishing Services.
10. Sieradzki, K & Newman, R.C. (1987). Stress-corrosion cracking. *J. Phys. Chem. Solids Vol. 48, No. 11, pp. 1101-1113*. Great Britain: Pergamon Journals Limited.
11. Lindley R. Higgins (1995). *Maintenance engineering handbook, 5th Edition*. United States of America: McGraw-Hill, Inc.

APPENDICES

Appendix 1 Wind load calculation per SANS 10160-1

All equations, figures and tables referenced below are taken from SANS 10160-1

Peak wind speed calculation, $v_p(z)$

$v_p(z) = c_r(z) \times c_o(z) \times v_{b,peak}$ per equation (3)

$v_b = 28m/s$, from Figure 1 of SANS 10160-1

$\therefore v_{b,peak} = 1.4 \times v_b = 1.4 \times 28 = 39.2m/s$ per equation (4)

$c_r(z) = 1.36 \times \frac{z-z_o}{z_g-z_c}^{\alpha}$, *z=31.84m*

$c_r(z) = 1.36 \times \frac{31.84-0}{300-2}^{0.095} = 1.1$ values obtained from Table1 per Terrain Category B

$c_o(z) = 1$

$\therefore v_p(z) = 1.1 \times 1 \times 39.2 = 43.12m/s$

Peak wind pressure calculation, $q_p(z)$

$q_p(z) = \frac{1}{2} \times \rho \times v_p^2(z)$

Given air density is 1.2 *kg/m*^{3} based on Table 4

$\therefore q_p(z) = 0.5 \times 1.2 \times 43.12^2 = 1116Pa$

Wind force calculation, F_w

$F_w = c_s \times c_d \times c_f \times q_p(z) \times A_{ref}$

Where,

$c_s c_d = 1$

$c_f = 0.7$

$A_{ref} = height \times mean\ diameter$, for the top section.

$\therefore F_w = 1 \times 0.7 \times 1116 \times 16.6 \times 6.8 = 88150N$

Appendix 2 Assessment for internal pressure, cylindrical section

All equations, figures and tables referenced below are taken from API 579-1 Annex A

Given information:

Internal Design Pressure	P	167kPa
Design temperature	T	350℃
Material of construction	HII	
Allowable stress of material	S	93.3MPa
Joint efficiency	E	0.85
Nominal thickness	t	19mm
Shell outside diameter	Do	6400mm
Shell inside diameter	Di	6362mm
Assessment thickness	tc	7.6mm
Weight of section above defect	F	1.16E06N
Moment from wind force	M	2.20E06Nm
Mean radius	Rm	3196.2mm

Calculated data:

$D_{corr} = 6362 + 2 * (6362 - 7.6) = 6384.8mm$

$R = \frac{D_{corr}}{2} = \frac{6384.8}{2} = 3192.4mm$

$check\ if\ P \leq 0.385SE, P \leq 0.385 * 93.3 * 0.85 \leq 30.5, ok$

Minimum thickness, circumferential stress

$t_{min}^{c} = \frac{PR}{SE - 0.6P} = \frac{0.167 * 3192.4}{93.3 * 0.85 - 0.6 * 0.167} = 6.7mm$

$check\ if\ t_{min}^{c} \leq 0.5R \leq 0.5 * 3192.4 \leq 1596.5, ok$

Membrane stress, circumferential stress

$\sigma_m^c = \frac{P}{E}\left(\frac{R}{t_c} + 0.6\right) = \frac{0.167}{0.85}\left(\frac{3192.4}{7.6} + 0.6\right) = 82.6MPa$

Minimum thickness, longitudinal stress

$t_{min}^{L} = \frac{PR}{2SE + 0.4P} + t_{sl}, where\ t_{sl}\ is\ thickness\ based\ on\ supplemental\ loading$

$t_{sl} = \frac{F}{2SE\pi R_m} + \frac{M}{SE\pi R_m^2} = \frac{1.16e6}{2 * 93.3 * 0.85 * \pi * 3196.2} + \frac{2.2e6}{93.3 * 0.85 * \pi * 3196.2^2} = 0.73mm$

$$t_{min}^{L} = \frac{PR}{2SE + 0.4P} + t_{sl} = \frac{0.167 * 3192.4}{2 * 93.3 * 085 + 0.4 * 0.167} + 0.73 = 4.1mm$$

Membrane stress, longitudinal stress

$$\sigma_m^L = \frac{P}{2E}\left(\frac{R}{t_c - t_{sl}} - 0.4\right) = \frac{0.167}{2 * 0.85}\left(\frac{3192.4}{7.6 - 0.73} - 0.4\right) = 45.6MPa$$

Final values,

$t_{min} = \max(t_{min}^{c}, t_{min}^{L}) = 6.7mm$

$\sigma_{max} = \max(\sigma_m^c, \sigma_m^L) = 82.6MPa$

Appendix 3 Buckling assessment, current condition

All equations, figures and tables referenced below are taken from API 579-1 Annex A

Given information:

Internal Design Pressure	P	167kPa
Design temperature	T	350℃
Material of construction	HII	
Allowable stress of material	S	93.3MPa
Yield strength	Sy	140MPa
Young's Modulus	Ey	187GPa
Joint efficiency	E	0.85
Nominal thickness	t	19mm
Shell outside diameter	Do	6400mm
Shell inside diameter	Di	6362mm
Assessment thickness	tc	7.6mm
Weight of section above defect	F	1.16E06N
Wind shear force	V	88150N
Moment from wind force	M	2.20E06Nm
Mean radius	Rm	3196.2mm
Unstiffened length	L,Lu	3100mm
Axial compression coefficient	Ku	2.1

Calculated data:

$D_{corr} = 6362 + 2 * (6362 - 7.6) = 6384.8mm$

Section Properties, Stresses, Buckling Parameters

$$A = \frac{\pi(D_o^2 - D^2)}{4} = \frac{\pi(6400^2 - 6384.8^2)}{4} = 152625.6mm^2$$

$$S = \frac{\pi(D_o^4 - D^4)}{32D_o} = \frac{\pi(6400^4 - 6384.8^4)}{32 * 6400} = 243621684.7mm^4$$

$$f_h = \frac{PD_o}{2t_c} = \frac{0.167 * 6400}{2 * 7.6} = 70.3MPa$$

$$f_b = \frac{M}{S} = \frac{2.2e6}{243621684.7} = 9.0MPa$$

$$f_a = \frac{F}{A} = \frac{1.16e6}{152625.6} = 7.6MPa$$

$$f_q = \frac{P\pi D^2}{4A} = \frac{0.167 * \pi * 6384.8^2}{4 * 152625.6} = 35MPa$$

$$f_v = \frac{V}{A} = \frac{88150}{152625.6} = 0.6MPa$$

$$r_g = 0.25\sqrt{D_o^2 + D^2} = 0.25\sqrt{6400^2} + 6384.8^2 = 2260.1mm$$

$$M_x = \frac{L}{\sqrt{R_o t_c}} = \frac{3100}{\frac{\sqrt{6400}}{2} * 7.6} = 19.9$$

1) External pressure acting alone, Fha

$$C_h = 1.12M_x^{-1.058} = 1.12 * 19.9^{-1.028} = 0.047$$

$$F_{he} = \frac{1.6C_h E_y t}{D_o} = \frac{1.6 * 0.047 * 187000 * 7.6}{6400} = 16.8MPa$$

$$F_{ic} = F_{he}, for\ \frac{F_{he}}{S_y} \leq 0.552$$

$$FS = 2.0, for\ F_{ic} \leq 0.55S_y$$

$$F_{ha} = \frac{F_{ic}}{FS} = \frac{16.8}{2} = 8.4MPa$$

$$P_a = 2F_{ha}\left(\frac{t}{D_o}\right) = 2 * 8.4 * \left(\frac{7.6}{6400}\right) = 0.020MPa$$

2) Axial compressive stress acting alone, Fxa

$$F_{xa1} = \frac{0.5S_y}{FS} = \frac{0.5 * 140}{2} = 35MPa$$

$$\bar{c} = 1.0, for\ M_x \geq 15$$

$$C_x = min\left[\frac{409\bar{c}}{\left(389 + \frac{D_o}{t}\right)}, 0.9\right] = min\left[\frac{409 * 1.0}{\left(389 + \frac{6400}{7.6}\right)}, 0.9\right] = 0.332$$

$$F_{xe} = \frac{C_x E_y t_c}{D_o} = \frac{0.332 * 187000 * 7.6}{6400} = 73.774MPa$$

$$F_{xa2} = \frac{F_{xe}}{FS} = \frac{73.774}{2} = 36.887MPa$$

$$F_{xa} = min[F_{xa1}, F_{xa2}] = 35MPa$$

$$\lambda_c = \frac{K_u L_u}{\pi r_g}\left(\frac{F_{xa} FS}{E_y}\right)^{0.5} = \frac{2.1 * 3100}{\pi * 2260.1}\left(\frac{35 * 2}{187000}\right)^{0.5} = 0.0177$$

3) Compressive bending stress, Fba

$$F_{ba} = F_{xa}, for\ 135 \leq \frac{D_o}{t_c} \leq 2000$$

4) Shear stress, Fva

$$C_v = \left(\frac{9.64}{M_x^2}\right)(1 + 0.0239M_x^3)^{0.5} = \left(\frac{9.64}{19.9^2}\right)(1 + 0.0239 * 19.9^3)^{0.5} = 0.3352$$

$$\alpha_v = 1.389 - 0.218\log_{10}\left(\frac{D_o}{t_c}\right) = 1.389 - 0.218 * \log_{10}\left(\frac{6400}{7.6}\right) = 0.751$$

$$F_{ve} = \alpha_v C_v E_y \left(\frac{t_c}{D_o}\right) = 0.751 * 0.3352 * 187000 * \left(\frac{7.6}{6400}\right) = 55.9MPa$$

$$\eta_v = 1.0, for\ \frac{F_{ve}}{S_y} \leq 0.48$$

$$F_{va} = \frac{\eta_v F_{ve}}{FS} = \frac{1.0 * 55.9}{2} = 27.96MPa$$

5) Axial compressive stress and hoop compression, Fxha

$$C_1 = \frac{(F_{xa}FS + F_{ha}FS)}{S_y} - 1.0 = \frac{(35 * 2 + 8.4 * 2)}{140} - 1.0 = -0.38$$

$$f_x = f_a + f_q = 7.6 + 35 = 42.66MPa$$

$$C_2 = \frac{f_x}{f_h} = \frac{42.66}{70.3} = 0.61$$

$$F_{xha} = \left[\left(\frac{1}{F_{xa}^2}\right) - \left(\frac{C_1}{C_2 F_{xa} F_{ha}}\right) + \left(\frac{1}{C_2^2 F_{ha}^2}\right)\right]^{-0.5}$$

$$= \left[\left(\frac{1}{35^2}\right) - \left(\frac{-0.38}{0.61 * 35 * 8.4}\right) + \left(\frac{1}{0.61^2 * 8.4^2}\right)\right]^{-0.5} = 4.92MPa, for\ \lambda_c \leq 0.15$$

$$F_{hxa} = \frac{F_{xha}}{C_2} = \frac{4.92}{0.61} = 8.11MPa, for\ \lambda_c \leq 0.15$$

6) Compressive bending stress and hoop compression, Fbha

$$n = 5 - \frac{4F_{ha}FS}{S_y} = \frac{4 * 8.4 * 2}{140} = 4.52$$

$$C_4 = \left(\frac{f_b}{f_h}\right)\left(\frac{F_{ha}}{F_{ba}}\right) = \left(\frac{9}{70.3}\right)\left(\frac{8.4}{35}\right) = 0.03094$$

$$C_3^2(C_4^2 + 0.6C_4) + C_3^{2n} - 1 = 0$$

Solving the above equation by iteration yields,

$$C_3 = 0.9978$$

$$F_{bha} = C_3 C_4 F_{ba} = 0.9978 * 0.03094 * 35 = 1.1MPa$$

$$F_{hba} = F_{bha}\left(\frac{f_h}{f_b}\right) = 1.1 * \left(\frac{70.3}{9}\right) = 8.4MPa$$

7) Shear stress and hoop compression, Fvha

$$C_5 = \frac{f_v}{f_h} = \frac{0.6}{70.3} = 0.008$$

$$F_{vha} = \left[\left(\frac{F_{va}^2}{2C_5F_{ha}}\right)^2 + F_{va}^2\right]^{0.5} - \frac{F_{va}^2}{2C_5F_{ha}} = \left[\left(\frac{27.96^2}{2 * 0.008 * 8.4}\right)^2 + 27.96^2\right]^{0.5} - \frac{27.96^2}{2 * 0.008 * 8.4}$$

$$= 0.069MPa$$

$$F_{hva} = \frac{F_{vha}}{C_5} = \frac{0.069}{0.008} = 8.4MPa$$

8) Axial compressive stress, compressive bending stress, shear stress, and hoop compression

$$K_s = 1.0 - \left(\frac{f_v}{F_{va}}\right)^2 = 1.0 - \left(\frac{0.6}{27.96}\right)^2 = 0.99957$$

$$\left(\frac{f_a}{K_sF_{xha}}\right)^{1.7} + \left(\frac{f_b}{K_sF_{bha}}\right) \leq 1.0$$

$$10.5 \leq 1.0, fail\ for\ \lambda_c \leq 0.15$$

9) Axial compressive stress, compressive bending stress and shear

$$\left(\frac{f_a}{K_sF_{xa}}\right)^{1.7} + \left(\frac{f_b}{K_sF_{ba}}\right) \leq 1.0$$

$$0.33364 \leq 1.0, pass\ for\ \lambda_c \leq 0.15$$

Appendix 4 Buckling assessment, additional stiffening ring

All equations, figures and tables referenced below are taken from API 579-1 Annex A

Given information:

Internal Design Pressure	P	167kPa
Design temperature	T	350℃
Material of construction	HII	
Allowable stress of material	S	93.3MPa
Yield strength	Sy	140MPa
Young's Modulus	Ey	187GPa
Joint efficiency	E	0.85
Nominal thickness	t	19mm
Shell outside diameter	Do	6400mm
Shell inside diameter	Di	6362mm
Assessment thickness	tc	7.6mm
Weight of section above defect	F	1.16E06N
Wind shear force	V	88150N
Moment from wind force	M	2.20E06Nm
Mean radius	Rm	3196.2mm
Unstiffened length	L,Lu	650mm
Axial compression coefficient	Ku	2.1

Calculated data:

$D_{corr} = 6362 + 2 * (6362 - 7.6) = 6384.8mm$

Section Properties, Stresses, Buckling Parameters

$$A = \frac{\pi(D_o^2 - D^2)}{4} = \frac{\pi(6400^2 - 6384.8^2)}{4} = 152625.6mm^2$$

$$S = \frac{\pi(D_o^4 - D^4)}{32D_o} = \frac{\pi(6400^4 - 6384.8^4)}{32 * 6400} = 243621684.7mm^4$$

$$f_h = \frac{PD_o}{2t_c} = \frac{0.167 * 6400}{2 * 7.6} = 70.3MPa$$

$$f_b = \frac{M}{S} = \frac{2.2e6}{243621684.7} = 9.0MPa$$

$$f_a = \frac{F}{A} = \frac{1.16e6}{152625.6} = 7.6MPa$$

$$f_q = \frac{P\pi D^2}{4A} = \frac{0.167 * \pi * 6384.8^2}{4 * 152625.6} = 35MPa$$

$$f_v = \frac{V}{A} = \frac{88150}{152625.6} = 0.6MPa$$

$$r_g = 0.25\sqrt{D_o^2 + D^2} = 0.25\sqrt{6400^2} + 6384.8^2 = 2260.1mm$$

$$M_x = \frac{L}{\sqrt{R_o t_c}} = \frac{650}{\frac{\sqrt{6400}}{2} * 7.6} = 4.2$$

1) External pressure acting alone, Fha

$$C_h = \frac{0.92}{M_x - 0.579} = \frac{0.92}{4.2 - 0.579} = 0.256$$

$$F_{he} = \frac{1.6 C_h E_y t}{D_o} = \frac{1.6 * 0.256 * 187000 * 7.6}{6400} = 91.1MPa$$

$$F_{ic} = F_{he}, for\ \frac{F_{he}}{S_y} \leq 0.552$$

$$FS = 2.0, for\ F_{ic} \leq 0.55 S_y$$

$$F_{ha} = \frac{F_{ic}}{FS} = \frac{91.1}{2} = 45.5MPa$$

$$P_a = 2F_{ha}\left(\frac{t}{D_o}\right) = 2 * 45.5 * \left(\frac{7.6}{6400}\right) = 0.108MPa$$

2) Axial compressive stress acting alone, Fxa

$$F_{xa1} = \frac{0.5 S_y}{FS} = \frac{0.5 * 140}{2} = 35MPa$$

$$\bar{c} = \frac{3.13}{M_x^{0,42}} = \frac{3.13}{4.2^{0,42}} = 1.72, for\ 1.5 \leq M_x \leq 15$$

$$C_x = min\left[\frac{409\bar{c}}{\left(389 + \frac{D_o}{t}\right)}, 0.9\right] = min\left[\frac{409 * 1.72}{\left(389 + \frac{6400}{7.6}\right)}, 0.9\right] = 0.571$$

$$F_{xe} = \frac{C_x E_y t_c}{D_o} = \frac{0.571 * 187000 * 7.6}{6400} = 126.8MPa$$

$$F_{xa2} = \frac{F_{xe}}{FS} = \frac{126.8}{2} = 63.4MPa$$

$$F_{xa} = min[F_{xa1}, F_{xa2}] = 35MPa$$

$$\lambda_c = \frac{K_u L_u}{\pi r_g}\left(\frac{F_{xa} FS}{E_y}\right)^{0.5} = \frac{2.1 * 650}{\pi * 2260.1}\left(\frac{35 * 2}{187000}\right)^{0.5} = 0.0037$$

3) Compressive bending stress, Fba

$$F_{ba} = F_{xa}, for\ 135 \leq \frac{D_o}{t_c} \leq 2000$$

4) Shear stress, Fva

$$C_v = \left(\frac{9.64}{M_x^2}\right)(1 + 0.0239M_x^3)^{0.5} = \left(\frac{9.64}{4.2^2}\right)(1 + 0.0239 * 4.2^3)^{0.5} = 0.9169$$

$$\alpha_v = 1.389 - 0.218\log_{10}\left(\frac{D_o}{t_c}\right) = 1.389 - 0.218 * \log_{10}\left(\frac{6400}{7.6}\right) = 0.751$$

$$F_{ve} = \alpha_v C_v E_y \left(\frac{t_c}{D_o}\right) = 0.751 * 0.9169 * 187000 * \left(\frac{7.6}{6400}\right) = 153MPa$$

$$\eta_v = 0.43\left(\frac{S_y}{F_{ve}}\right) + 0.1 = 0.43\left(\frac{140}{153}\right) + 0.1 = 0.494, for\ 0.48 \leq \frac{F_{ve}}{S_y} \leq 1.7$$

$$F_{va} = \frac{\eta_v F_{ve}}{FS} = \frac{0.494 * 153}{2} = 37.75MPa$$

5) Axial compressive stress and hoop compression, Fxha

$$C_1 = \frac{(F_{xa}FS + F_{ha}FS)}{S_y} - 1.0 = \frac{(35 * 2 + 45.5 * 2)}{140} - 1.0 = 0.15$$

$$f_x = f_a + f_q = 7.6 + 35 = 42.66MPa$$

$$C_2 = \frac{f_x}{f_h} = \frac{42.66}{70.3} = 0.61$$

$$F_{xha} = \left[\left(\frac{1}{F_{xa}^2}\right) - \left(\frac{C_1}{C_2 F_{xa} F_{ha}}\right) + \left(\frac{1}{C_2^2 F_{ha}^2}\right)\right]^{-0.5}$$

$$= \left[\left(\frac{1}{35^2}\right) - \left(\frac{0.15}{0.61 * 35 * 45.5}\right) + \left(\frac{1}{0.61^2 * 45.5^2}\right)\right]^{-0.5} = 22.53MPa, for\ \lambda_c \leq 0.15$$

$$F_{hxa} = \frac{F_{xha}}{C_2} = \frac{22.53}{0.61} = 37.13MPa, for\ \lambda_c \leq 0.15$$

6) Compressive bending stress and hoop compression, Fbha

$$n = 5 - \frac{4F_{ha}FS}{S_y} = \frac{4 * 45.5 * 2}{140} = 2.4$$

$$C_4 = \left(\frac{f_b}{f_h}\right)\left(\frac{F_{ha}}{F_{ba}}\right) = \left(\frac{9}{70.3}\right)\left(\frac{45.5}{35}\right) = 0.167$$

$$C_3^2(C_4^2 + 0.6C_4) + C_3^{2n} - 1 = 0$$

Solving the above equation by iteration yields,

$$C_3 = 0.97335$$

$$F_{bha} = C_3 C_4 F_{ba} = 0.97335 * 0.167 * 35 = 5.7MPa$$

$$F_{hba} = F_{bha}\left(\frac{f_h}{f_b}\right) = 5.7 * \left(\frac{70.3}{9}\right) = 44.3MPa$$

7) Shear stress and hoop compression, Fvha

$$C_5 = \frac{f_v}{f_h} = \frac{0.6}{70.3} = 0.008$$

$$F_{vha} = \left[\left(\frac{F_{va}^2}{2C_5 F_{ha}}\right)^2 + F_{va}^2\right]^{0.5} - \frac{F_{va}^2}{2C_5 F_{ha}} = \left[\left(\frac{37.75^2}{2 * 0.008 * 45.5}\right)^2 + 37.75^2\right]^{0.5} - \frac{37.75^2}{2 * 0.008 * 45.5}$$

$$= 0.374MPa$$

$$F_{hva} = \frac{F_{vha}}{C_5} = \frac{0.374}{0.008} = 45.5MPa$$

8) Axial compressive stress, compressive bending stress, shear stress, and hoop compression

$$K_s = 1.0 - \left(\frac{f_v}{F_{va}}\right)^2 = 1.0 - \left(\frac{0.6}{27.96}\right)^2 = 0.99957$$

$$\left(\frac{f_a}{K_s F_{xha}}\right)^{1.7} + \left(\frac{f_b}{K_s F_{bha}}\right) \leq 1.0$$

$$1.75 \leq 1.0, fail\ for\ \lambda_c \leq 0.15$$

9) Axial compressive stress, compressive bending stress and shear

$$\left(\frac{f_a}{K_s F_{xa}}\right)^{1.7} + \left(\frac{f_b}{K_s F_{ba}}\right) \leq 1.0$$

$$0.33364 \leq 1.0, pass\ for\ \lambda_c \leq 0.15$$

Appendix 5 External pressure, design conditions

All equations, figures and tables referenced below are taken from API 579-1 Annex A

Given information:

Internal Design Pressure	P	167kPa
Design temperature	T	350℃
Material of construction	HII	
Allowable stress of material	S	93.3MPa
Yield strength	Sy	140MPa
Young's Modulus	Ey	187GPa
Joint efficiency	E	0.85
Nominal thickness	t	19mm
Shell outside diameter	Do	6400mm
Shell inside diameter	Di	6362mm
Assessment thickness	tc	15mm
Weight of section above defect	F	1.16E06N
Wind shear force	V	88150N
Moment from wind force	M	2.20E06Nm
Mean radius	Rm	3196.2mm
Unstiffened length	L,Lu	650mm
Axial compression coefficient	Ku	2.1

Calculated data:

$D_{corr} = 6362 + 2 * (6362 - 7.6) = 6384.8mm$

Section Properties, Stresses, Buckling Parameters

$$A = \frac{\pi(D_o^2 - D^2)}{4} = \frac{\pi(6400^2 - 6384.8^2)}{4} = 152625.6mm^2$$

$$S = \frac{\pi(D_o^4 - D^4)}{32D_o} = \frac{\pi(6400^4 - 6384.8^4)}{32 * 6400} = 243621684.7mm^4$$

$$f_h = \frac{PD_o}{2t_c} = \frac{0.167 * 6400}{2 * 7.6} = 70.3MPa$$

$$f_b = \frac{M}{S} = \frac{2.2e6}{243621684.7} = 9.0MPa$$

$$f_a = \frac{F}{A} = \frac{1.16e6}{152625.6} = 7.6MPa$$

$$f_q = \frac{P\pi D^2}{4A} = \frac{0.167 * \pi * 6384.8^2}{4 * 152625.6} = 35MPa$$

$$f_v = \frac{V}{A} = \frac{88150}{152625.6} = 0.6MPa$$

$$r_g = 0.25\sqrt{D_o^2} + D^2 = 0.25\sqrt{6400^2} + 6384.8^2 = 2260.1mm$$

$$M_x = \frac{L}{\sqrt{R_o t_c}} = \frac{650}{\frac{\sqrt{6400}}{2} * 15} = 14.1$$

1) External pressure acting alone, Fha

$$C_h = 1.12M_x^{-1.058} = 1.12 * 4.2^{-1.028} = 0.068$$

$$F_{he} = \frac{1.6C_h E_y t}{D_o} = \frac{1.6 * 0.068 * 187000 * 15}{6400} = 47.6MPa$$

$$F_{ic} = F_{he}, for\ \frac{F_{he}}{S_y} \leq 0.552$$

$$FS = 2.0, for\ F_{ic} \leq 0.55S_y$$

$$F_{ha} = \frac{F_{ic}}{FS} = \frac{47.6}{2} = 23.8MPa$$

$$P_a = 2F_{ha}\left(\frac{t}{D_o}\right) = 2 * 23.8 * \left(\frac{15}{6400}\right) = 0.112MPa$$